JACS
JOURNAL OF THE AMERICAN CHEMICAL SOCIETY
pubs.acs.org/JACS
Communication

Chemoproteomic Identification of Blue-Light-Damaged Proteins

Kohei Toh, Kosuke Nishio, Reiko Nakagawa, Syusuke Egoshi, Masahiro Abo, Amelie Perron, Shin-ichi Sato, Naoki Okumura, Noriko Koizumi, Kosuke Dodo, Mikiko Sodeoka, and Motonari Uesugi*

Cite This: J. Am. Chem. Soc. 2022, 144, 20171−20176
Read Online

ABSTRACT: Visible light, particularly in the blue region of the spectrum, can cause cell dysfunction through the generation of singlet oxygen, contributing to cellular aging and age-related pathologies. Although photooxidation of nucleic acids, lipids, and amino acids has been extensively studied, the magnitude and span of blue-light-induced protein damages within proteome remain largely unknown. Herein we present a chemoproteomic approach to mapping blue-light-damaged proteins in live mammalian cells by exploiting a nucleophilic alkyne chemical probe. A gene ontology enrichment analysis revealed that cell surface proteins are more readily oxidized than other susceptible sets of proteins, including mitochondrial proteins. In particular, the integrin family of cell surface receptors (ITGs) was highly ranked in the mammalian cells tested, including human corneal endothelial cells. The blue-light-oxidized ITGB1 protein was functionally inactive in promoting cell adhesion and proliferation, suggesting that the photodamage of integrins contributes to the blue-light-induced cell dysfunction. Further application of our method to various cells and tissues should lead to a comprehensive analysis of light-sensitive proteins.

Light exposure is generally detrimental to human cells. Although visible light has widely been exploited in biological sciences, especially in optogenetics[1] and super-resolution imaging,[2] its irradiation can cause cell dysfunction.[3] The blue region (400−500 nm) of the visible spectrum is particularly important because it has a relatively high energy and is associated with the occurrence of cellular aging and age-related pathologies.[4,5] Blue-light irradiation causes the oxidation of nucleic acids, lipids, and proteins by generating singlet oxygen ($^1O_2$),[6] superoxides,[7] and hydrogen peroxide (H_2O_2)[3,6] through blue-light-absorbing endogenous photosensitizers including flavins,[8] porphyrins,[9] and melanin.[10] Such oxidative stress often modulates intracellular signals,[11] and excessive exposure to blue light causes cell death.[12] Toward an understanding of the underlying mechanism, the oxidation of biomolecules by $^1O_2$ has been intensely studied. In nucleic acids, guanine appears to be particularly susceptible to oxidation, as exemplified by the $^1O_2$ oxidation of the guanine tracts found in the G4 quadruplex structures of telomeres.[13] In lipids, the primary targets are those with unsaturated double bonds, such as retinoids, cholesterol, and phospholipids.[6] In the case of proteins, tyrosine, histidine, methionine, cysteine, and tryptophan are known to be oxidized by blue-light exposure.[6] However, the magnitude and span of blue-light-induced protein damages within a proteome remain largely unknown. This is in part due to the lack of a systematic and simple analytical methodology.

Chemoproteomics, in which the cellular proteome is labeled and identified with chemical probes, have attracted attention as a robust approach to interrogating the functional states of cellular proteins.[14−18] On the other hand, the Nakamura[19] and Hamachi[20] groups have recently reported proximal labeling of selective proteins by combining $^1O_2$-generating protein ligands and nitrogen-containing nucleophilic probes. Inspired by these seminal studies, we postulated that it might be possible to capture and analyze blue-light-oxidized intracellular proteins with nitrogen-containing nucleophilic probes at proteome levels.

Chemical probes suitable for proteome analysis need to combine cell permeability, moderate reactivity, and selectivity. Although the probes developed by Nakamura and Hamachi are suitable for selective proximal labeling of proteins, their electron-rich aromatic properties may also lead to the modification of nucleophilic amino acids upon oxidation.[21,22] To explore probes suitable for photooxidative proteomic analysis, we set out to screen nonaromatic, low-molecular-weight alkyne amine probes. The workflow for the screening is shown in Figure 1A. Proteomic lysates of HeLa cells were irradiated with blue light (450 nm, 14 mW) for 10 min in the presence of a nitrogen-containing nucleophilic probe and flavin mononucleotide (FMN), an intracellular photosensitizer. Labeled proteins were visualized by a click reaction with the fluorescent dye TAMRA azide. Fluorescence scanning of SDS-PAGE gels showed that probes **1** and **2** had comparable levels of protein labeling (Figure 1B). Secondary and tertiary amine versions of probe **1** (probes **4** and **5**) displayed lower levels of labeling than probe **1** (Figure S1). Next, we compared probes **1**−**3** in live cells. HeLa cells were maintained in DMEM, which contains riboflavin, and subsequently irradiated by blue light (450 nm, 14 mW) in EBSS, a medium lacking riboflavin. Surprisingly, the simplest probe, probe **1**, displayed the highest

Received: July 8, 2022
Published: October 28, 2022

https://doi.org/10.1021/jacs.2c07180
J. Am. Chem. Soc. 2022, 144, 20171−20176

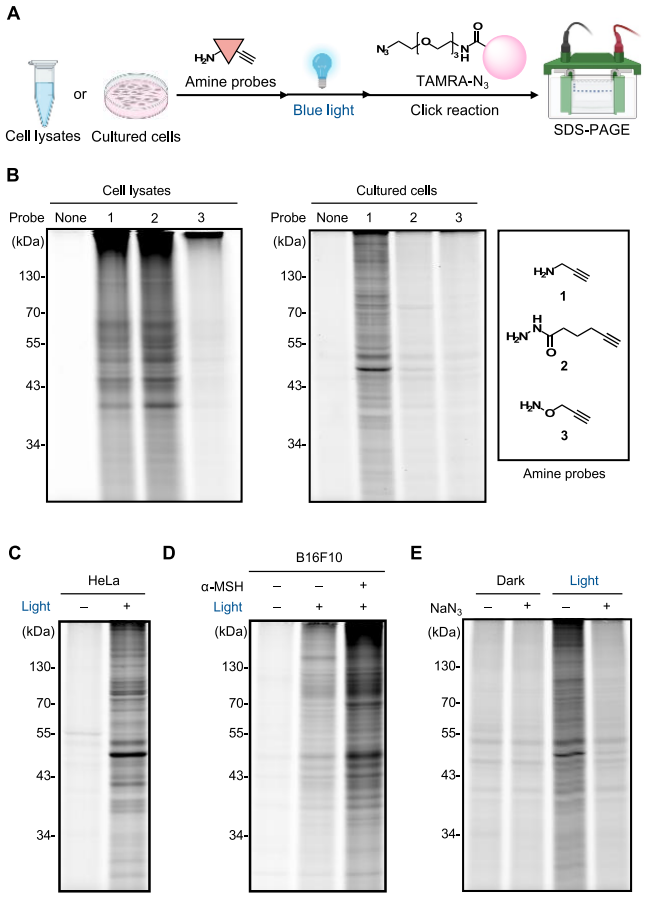

Figure 1. Proteome labeling with amine probes under blue light irradiation. (A) Workflow of the probe screening. (B) Fluorescence scanning of SDS-PAGE gels. HeLa cell lysates or cultured HeLa cells were exposed to each amine probe (2 mM) prior to blue-light irradiation for 10 min. Labeled proteins were reacted with TAMRA-N_3 by a click reaction and separated by SDS-PAGE. (C, D) Blue-light-dependent protein labeling with probe **1**. HeLa (C) or B16F10 (D) cells were treated with probe **1** in the presence or absence of blue-light irradiation. (E) Effect of NaN_3 (10 mM) on the protein labeling with probe **1**.

levels of labeling (Figure 1B). The difference between the *in vitro* and *in cellulo* results may be due to distinct levels of cell permeability of the probes. These results indicate that, of the probes screened, probe **1** is the most suitable for further proteome analysis in living cells. To rule out the possibility that the blue-light-activated probe **1** reacted with nonoxidized proteins, we preirradiated the probe and added it to HeLa cell lysates (Figure S2). The preirradiated probe displayed protein labeling as low as the nonirradiated sample did, supporting our notion that the labeled proteins represent blue-light-damaged proteins.

The protein labeling by probe **1** in HeLa cells was blue-light-dependent, with little protein labeling without blue light (Figure 1C and Figures S3A and S4). We selected 10 min blue light exposure (450 nm, 14 mW) in the presence of 2 mM probe **1** as a labeling condition for later studies (Figure S4). When B16F10 pigment cells were used, a higher level of protein labeling was observed upon the addition of α-MSH, a hormone that stimulates melanin biosynthesis (Figure 1D and Figure S3B,C). To verify whether such intracellular protein labeling is mediated by endogenous photosensitizers, we performed *in vitro* labeling experiments using BSA as a model protein. The addition of flavin derivatives or melanin increased the probe **1** labeling of BSA in a light-dependent manner (Figure S5A,B). Porphyrin derivatives had little effect on the levels of BSA labeling (Figure S5A). Importantly, NaN_3, a singlet oxygen quencher, canceled the protein labeling *in vitro* and in HeLa cells (Figure 1E and Figure S5C). Taken together, the blue light-induced cellular protein labeling by probe **1** is likely to be mediated primarily by $^1O_2$ generated from photoactivated flavin derivatives and/or melanin.

To identify blue-light-oxidized proteins, we performed a chemoproteomic LC-MS/MS analysis as outlined in Figure 2A. Cells were treated with probe **1** under blue-light irradiation

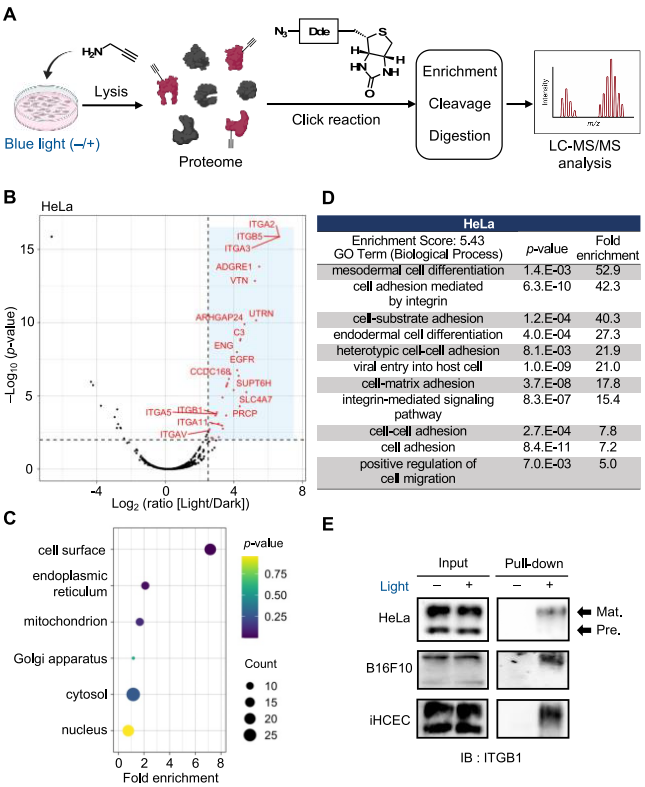

Figure 2. LC-MS/MS analysis of blue-light-oxidized proteins. (A) Workflow of the proteomic analysis. Cells were treated with probe **1** (2 mM) and blue light (10 min) prior to a click reaction with Dde-biotin azide. The biotinylated proteins were enriched by streptavidin agarose resins, eluted by N_2H_4, and trypsinized before LS-MS/MS analysis. (B) Volcano plots (ratio [Light/Dark] vs p value) of HeLa cells. Highly oxidized proteins (HOPs, $\log_2$[Light/Dark] > 2.5, p value <0.01) are indicated as red dots. (C) Subcellular localization of HOPs in HeLa cells. GO enrichment analysis (cellular component) was conducted for the 98 HOPs. (D) Functional annotation clustering (biological process) of the HOPs. (E) Pull-down and Western blot analysis of ITGB1 in HeLa, B16F10, and iHCEC cells after blue light irradiation for 10 min with probe **1** (2 mM). Abbreviations: Mat., mature; Pre., precursor.

for 10 min, lysed, and reacted with Dde-biotin azide, a biotinylated click reagent whose linker is readily cleaved by N_2H_4.[23] The biotinylated proteins were isolated by avidin agarose, eluted by N_2H_4, and analyzed by LC-MS/MS for label-free quantification.[24] In HeLa and B16F10 cells, the numbers of highly oxidized proteins (HOPs, $\log_2$[Light/Dark] > 2.5 and p value <0.01) were 98 and 131, respectively (Figure 2B and Figure S6A) (see also Supporting Excel files 1 and 2).

https://doi.org/10.1021/jacs.2c07180
J. Am. Chem. Soc. 2022, 144, 20171−20176

A gene ontology (GO) enrichment analysis of HOPs in both HeLa and B16F10 cells revealed that cell surface proteins were more readily oxidized than proteins located in other organelles (Figure 2C and Figure S6B). This finding was unexpected, since photooxidation is believed to occur primarily in mitochondria, where flavin enzymes are abundant.[3] To exclude the possibility that the preferential labeling of cell surface proteins was due to the limited cell permeability of the probe, we conducted Raman microscopy experiments, which permitted selective detection of an alkyne group in living cells (Figure S7).[25,26] The Raman signals of the free and protonated forms of probe **1** at 2119 and 2139 cm^{-1}, respectively, were found more abundantly in the intracellular region than in the extracellular space.

Functional annotation clustering of GO biological process of the HOPs revealed that cell adhesion, in particular mediated by integrins, exhibited high enrichment scores in both HeLa and B16F10 cells (Figure 2D and Figure S6E). To corroborate this finding in more physiologically relevant cells, we expanded the analysis to human corneal endothelial cells (iHCEC) (Supporting Excel file 3). The cornea is the first tissue in the eye to be exposed to external light. In the blue-light-exposed cornea cells, cell surface proteins were again highly oxidized, and integrin-mediated cell adhesion gave the highest enrichment scores (Figure S6C–E). These results collectively suggest that the integrin family members are sensitive to blue-light irradiation.

For an in-depth functional analysis, we focused on integrin β1 (ITGB1), a major and well-characterized player of the integrin family that was highly oxidized in HeLa, B16F10, and iHCEC cells. The blue-light-dependent labeling of ITGB1 was confirmed by a Western blot analysis of the probe-labeled proteins from HeLa, B16F10, and iHCEC cells (Figure 2E). Two ITGB1 bands were detected in the input samples of HeLa and iHCEC cells: the upper band corresponds to the mature, glycosylated form of ITGB1 located on the cell surface.[27] Interestingly, the cell-surface form of ITGB1 was selectively labeled by probe **1**, consistent with the results of the GO analysis.

ITGB1 is a cell-surface protein that forms heterodimers with integrin α family members to control cell adhesion, migration, and survival.[28] Upon binding to the ECM, ITGB1 undergoes a conformational change from bent to extended forms, thereby clustering intracellular adaptor proteins to induce phosphorylation of focal adhesion kinase (FAK) (Figure 3A).[29] To examine the effects of blue-light irradiation on the activation status of ITGB1, we performed immunostaining with a 12G10 antibody, which specifically marked the activated, extended ITGB1 forms.[30] The results revealed that blue-light exposure decreased the number of the activated forms of ITGB1 to ~30% (Figure 3B). In contrast, addition of H_2O_2 (1 mM) had little effect on the ITGB1 conformation (Figure S8), suggesting that a reactive oxygen species other than H_2O_2, most likely $^1O_2$, plays a role in the ITGB1 damage.

In line with the immunostaining, the blue-light exposure suppressed the phosphorylation of FAK in the HeLa cells cultured on the plate coated with each of the three different integrin-activating ECMs fibronectin, collagen I, or laminin, while it had little effects on the protein levels of ITGB1 (Figure 3C). Moreover, when the blue-light-irradiated cells were reseeded on the plates coated with each ECM, the number of adhered cells significantly decreased to ~10% compared with nonirradiated cells (Figure 3D and Figure S9). Addition

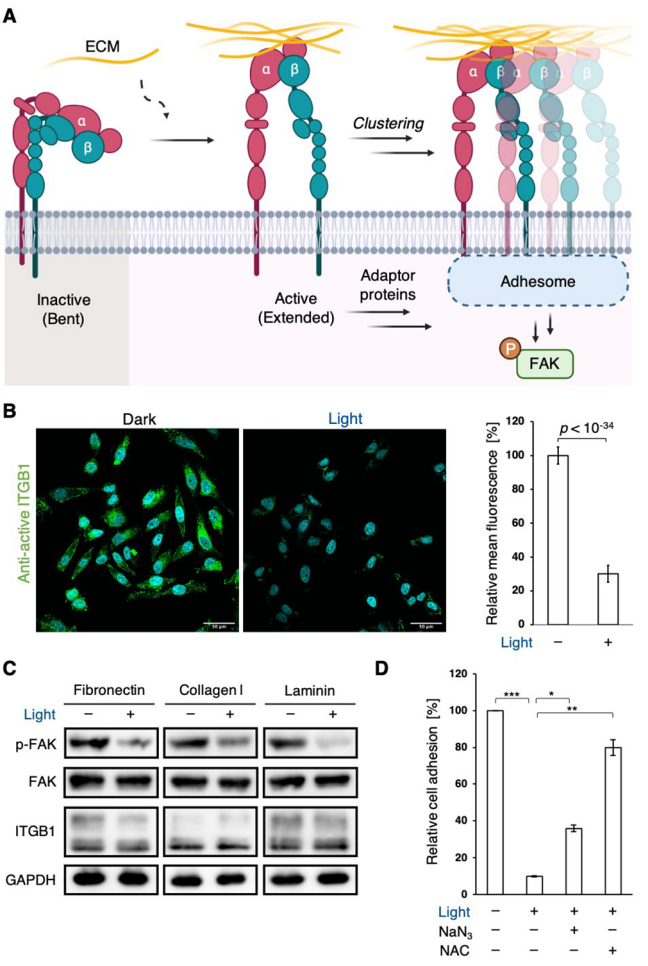

Figure 3. Analysis of ITGB1 function after blue-light irradiation. (A) Cartoon of ITGB1 activation and downstream signaling. (B) Immunostaining of active ITGB1 in blue-light-irradiated (Light) and nonirradiated (Dark) HeLa cells. Color code: green, active ITGB1; cyan, Hoechst 33342. The values represent the mean of fluorescence ± SD (n = 53 in Dark; n = 64 in Light). Significance was determined using an unpaired two-tailed Student's t-test. (C) Western blot analysis of FAK phosphorylation in HeLa cells after blue-light irradiation for 10 min. (D) Effect of blue-light irradiation on cell adhesion. HeLa cells were reseeded on Collagen I coated plates after blue-light irradiation for 10 min. Experiments were replicated in triplicate. Data represent average ± SD. Significance was determined using an unpaired two-tailed Student's t-test: $*p < 10^{-3}$; $**p < 10^{-4}$; $***p < 10^{-5}$.

of a singlet oxygen quencher, NaN_3 or N-acetyl cysteine (NAC), mitigated the compromised adhesion of cells. In particular, NAC (2 mM) almost completely blocked the probe labeling (Figure S10) and restored the adhesion of the blue-light-irradiated HeLa cells (Figure 3D). Overall, these results suggest that blue-light-induced $^1O_2$ oxidizes ITGB1, thus blunting its ability to stimulate the ECM-dependent downstream signaling.

Next, we attempted to map the amino acid residues oxidized by blue-light exposure. An analysis of the amino acid residues of BSA photolabeled with probe **1** showed histidines and tyrosines as conjugation sites (Figures S11 and S12). Blue-light exposure of Fmoc-tyrosine or Fmoc-histidine in the presence of probe **1** generated a conjugated product whose molecular weight is consistent with the expected oxidized product (Scheme S1 and Figure S13). These results confirmed that

https://doi.org/10.1021/jacs.2c07180
J. Am. Chem. Soc. 2022, 144, 20171−20176

probe **1** detects the photooxidation of histidines and tyrosines. To estimate which histidines and tyrosines in ITGB1 are oxidized by blue-light irradiation, we treated HeLa cells overexpressing c-Myc-tagged ITGB1 with blue light for 10 min and used LC-MS/MS to analyze the oxidation status of trypsinized peptides from immune-purified c-Myc-tagged ITGB1 (Figure S14). As a result, Y153, Y345, Y783, and H690 were found to be significantly oxidized in blue-light-irradiated samples (Figure S15) (Supporting Excel file 4). Among them, Y783 has been reported to play an important role in the downstream signaling of ITGB1.[31,32] However, other functionally important tyrosines and histidines might be photo-oxidized in light of the low coverage of the sequenced peptides (56%) (Figure S16). How the oxidations of histidine and/or tyrosine oxidations affect the function of ITGB1 remains unclear.

The present study shows that ITGB1 is poised to be inactivated in mammalian cells, including human corneal endothelial cells, following exposure to blue light. In eye tissues, the cornea is the first to be exposed to blue light emitted by sunlight and electronic devices, thereby being subject to photooxidative stress.[33] Excessive oxidative stress in corneal endothelial cells is considered to cause Fuchs' corneal dystrophy, an ophthalmology disease leading to vision loss.[34] The major integrin heterodimers in corneal endothelial cells are $\alpha3\beta1$ and $\alpha6\beta1$, which bind to laminin in Descemet's membrane to activate downstream signaling.[35,36] Although ITGB1 damage has not been reported to contribute to corneal disease, ITGB1 conditional knockout mice in keratocytes and lens cells have been shown to lose the structural integrity of the cornea and lens tissue.[37,38] ITGB1 is likely to engage in the maintenance of a healthy cornea and lens. How the photodamage of ITGB1 and other integrin family members contributes to the light-induced ocular tissue damage and how it can pharmacologically be restored remains to be investigated.

Another revelation by our study is that the probe that best captured photo-oxidized proteins was a simple primary amine. A range of primary amine molecules, including lysine, monoamines, and polyamines, are present inside and outside the cells. Our findings suggest that these cellular amines might also nonenzymatically modify photo-oxidized proteins. Whether photo-oxidized ITGB1 is modified by endogenous amines remains to be elucidated.

A weakness of our method is that it can detect the photodamaged side chains of only limited amino acids, tyrosine and histidine residues. The development of oxidation-dependent probes selective for other amino acids would facilitate the study of photodamaged proteins. Nevertheless, given that tyrosine and histidine are often functionally important, the method may enable us to pinpoint photo-damaged proteins whose biological functions are modulated, as exemplified by our case study of ITGB1. Another limitation of our method is that cells were exposed to 14 mW blue light for 10 min. This intense exposure produces an acute damage to cellular proteins, which does not necessarily recapture the slow aging process of cellular proteins under much weaker daily light conditions. The proteomic dissection of aging-related pathologies requires experimental conditions that more faithfully reproduce the daily light-induced chronic aging process. Nevertheless, further application of our method to various cells and tissues should lead to a comprehensive analysis of light-sensitive proteins.

■ ASSOCIATED CONTENT

Supporting Information

The Supporting Information is available free of charge at https://pubs.acs.org/doi/10.1021/jacs.2c07180.

Supplemental figures as described in the text, proteomic data, and experimental details (PDF)

HeLa proteomics data (XLSX)

B16F10 proteomics data (XLSX)

iHCEC proteomics data (XLSX)

Peptide sequence data from LC-MS/MS analysis of photodamaged ITGB1 (XLSX)

■ AUTHOR INFORMATION

Corresponding Author

Motonari Uesugi − *Institute for Chemical Research, Kyoto University, Uji, Kyoto 611-0011, Japan; Institute for Integrated Cell-Material Sciences (WPI-iCeMS), Kyoto University, Uji, Kyoto 611-0011, Japan; School of Pharmacy, Fudan University, Shanghai 201203, People's Republic of China;* orcid.org/0000-0002-8515-445X; Email: uesugi@scl.kyoto-u.ac.jp

Authors

Kohei Toh − *Institute for Chemical Research, Kyoto University, Uji, Kyoto 611-0011, Japan*

Kosuke Nishio − *Institute for Chemical Research, Kyoto University, Uji, Kyoto 611-0011, Japan*

Reiko Nakagawa − *Laboratory for Cell-Free Protein Synthesis, RIKEN Center for Biosystems Dynamics Research, Kobe, Hyogo 650-0047, Japan*

Syusuke Egoshi − *Synthetic Organic Chemistry Laboratory, RIKEN Cluster for Pioneering Research, Wako, Saitama 351-0198, Japan; Catalysis and Integrated Research Group, RIKEN Center for Sustainable Resource Science, Wako, Saitama 351-0198, Japan*

Masahiro Abo − *Institute for Chemical Research, Kyoto University, Uji, Kyoto 611-0011, Japan*

Amelie Perron − *Institute for Chemical Research, Kyoto University, Uji, Kyoto 611-0011, Japan; Institute for Integrated Cell-Material Sciences (WPI-iCeMS), Kyoto University, Uji, Kyoto 611-0011, Japan*

Shin-ichi Sato − *Institute for Chemical Research, Kyoto University, Uji, Kyoto 611-0011, Japan;* orcid.org/0000-0003-3085-419X

Naoki Okumura − *Department of Biomedical Engineering, Faculty of Life and Medical Sciences, Doshisha University, Kyotanabe, Kyoto 610-0321, Japan*

Noriko Koizumi − *Department of Biomedical Engineering, Faculty of Life and Medical Sciences, Doshisha University, Kyotanabe, Kyoto 610-0321, Japan*

Kosuke Dodo − *Synthetic Organic Chemistry Laboratory, RIKEN Cluster for Pioneering Research, Wako, Saitama 351-0198, Japan; Catalysis and Integrated Research Group, RIKEN Center for Sustainable Resource Science, Wako, Saitama 351-0198, Japan;* orcid.org/0000-0001-6008-2915

Mikiko Sodeoka − *Synthetic Organic Chemistry Laboratory, RIKEN Cluster for Pioneering Research, Wako, Saitama 351-0198, Japan; Catalysis and Integrated Research Group, RIKEN Center for Sustainable Resource Science, Wako, Saitama 351-0198, Japan;* orcid.org/0000-0002-1344-364X

Complete contact information is available at: https://pubs.acs.org/10.1021/jacs.2c07180

Notes

The authors declare no competing financial interest.

■ ACKNOWLEDGMENTS

This work was supported in part by JSPS (21K19045 and 22H00350 to M.U.), JST CREST (Grant Number JPMJCR1925 to M.S.), JST (the establishment of university fellowships towards the creation of science technology innovation; JPMJFS2123 to K.T.), and Kyoto University on-site lab program "Kyoto University Shanghai Lab". The authors thank F. A. Quiocho for critical reading. Generalized figures were created using Biorender. This work was inspired by the international and interdisciplinary environments of the JSPS CORE-to-CORE Program "Asian Chemical Biology Initiative".

■ REFERENCES

(1) Mansouri, M.; Strittmatter, T.; Fussenegger, M. Light-Controlled Mammalian Cells and Their Therapeutic Applications in Synthetic Biology. *Adv. Sci.* **2019**, *6* (1), 1800952.

(2) Cox, S.; Rosten, E.; Monypenny, J.; Jovanovic-Talisman, T.; Burnette, D. T.; Lippincott-Schwartz, J.; Jones, G. E.; Heintzmann, R. Bayesian Localisation Microscopy Reveals Nanoscale Podosome Dynamics. *Nat. Methods* **2012**, *9* (2), 195−200.

(3) Godley, B. F.; Shamsi, F. A.; Liang, F.-Q.; Jarrett, S. G.; Davies, S.; Boulton, M. Blue Light Induces Mitochondrial DNA Damage and Free Radical Production in Epithelial Cells. *J. Biol. Chem.* **2005**, *280* (22), 21061−21066.

(4) Alaimo, A.; Liñares, G. G.; Bujjamer, J. M.; Gorojod, R. M.; Alcon, S. P.; Martínez, J. H.; Baldessari, A.; Grecco, H. E.; Kotler, M. L. Toxicity of Blue Led Light and A2E Is Associated to Mitochondrial Dynamics Impairment in ARPE-19 Cells: Implications for Age-Related Macular Degeneration. *Arch. Toxicol.* **2019**, *93* (5), 1401−1415.

(5) Nash, T. R.; Chow, E. S.; Law, A. D.; Fu, S. D.; Fuszara, E.; Bilska, A.; Bebas, P.; Kretzschmar, D.; Giebultowicz, J. M. Daily Blue-Light Exposure Shortens Lifespan and Causes Brain Neurodegeneration in Drosophila. *Npj Aging Mech Dis* **2019**, *5* (1), 8.

(6) Di Mascio, P.; Martinez, G. R.; Miyamoto, S.; Ronsein, G. E.; Medeiros, M. H. G.; Cadet, J. Singlet Molecular Oxygen Reactions with Nucleic Acids, Lipids, and Proteins. *Chem. Rev.* **2019**, *119* (3), 2043−2086.

(7) Foote, C. S. Mechanisms of Photosensitized Oxidation. *Science* **1968**, *162* (3857), 963−970.

(8) Yang, M.-Y.; Chang, C.-J.; Chen, L.-Y. Blue Light Induced Reactive Oxygen Species from Flavin Mononucleotide and Flavin Adenine Dinucleotide on Lethality of HeLa Cells. *J. Photochem. Photobiology B Biology* **2017**, *173*, 325−332.

(9) Buglak, A. A.; Filatov, M. A.; Hussain, M. A.; Sugimoto, M. Singlet Oxygen Generation by Porphyrins and Metalloporphyrins Revisited: A Quantitative Structure-Property Relationship (QSPR) Study. *J. Photochem. Photobiology Chem.* **2020**, *403*, 112833.

(10) Chiarelli-Neto, O.; Pavani, C.; Ferreira, A. S.; Uchoa, A. F.; Severino, D.; Baptista, M. S. Generation and Suppression of Singlet Oxygen in Hair by Photosensitization of Melanin. *Free Radical Bio Med.* **2011**, *51* (6), 1195−1202.

(11) Klotz, L.-O.; Kröncke, K.-D.; Sies, H. Singlet Oxygen-Induced Signaling Effects in Mammalian Cells. *Photochem. Photobio S* **2003**, *2* (2), 88−94.

(12) Huang, C.; Zhang, P.; Wang, W.; Xu, Y.; Wang, M.; Chen, X.; Dong, X. Long-Term Blue Light Exposure Induces RGC-5 Cell Death in Vitro: Involvement of Mitochondria-Dependent Apoptosis, Oxidative Stress, and MAPK Signaling Pathways. *Apoptosis* **2014**, *19* (6), 922−932.

(13) Fleming, A. M.; Chabot, M. B.; Nguyen, N. L. B.; Burrows, C. J. Collateral Damage Occurs When Using Photosensitizer Probes to Detect or Modulate Nucleic Acid Modifications. *Angewandte Chemie Int. Ed* **2022**, *61* (7), No. e202110649.

(14) Matthews, M. L.; He, L.; Horning, B. D.; Olson, E. J.; Correia, B. E.; Yates, J. R.; Dawson, P. E.; Cravatt, B. F. Chemoproteomic Profiling and Discovery of Protein Electrophiles in Human Cells. *Nat. Chem.* **2017**, *9* (3), 234−243.

(15) Chuh, K. N.; Pratt, M. R. Chemical Methods for the Proteome-Wide Identification of Posttranslationally Modified Proteins. *Curr. Opin Chem. Biol.* **2015**, *24*, 27−37.

(16) Tate, E. W.; Kalesh, K. A.; Lanyon-Hogg, T.; Storck, E. M.; Thinon, E. Global Profiling of Protein Lipidation Using Chemical Proteomic Technologies. *Curr. Opin Chem. Biol.* **2015**, *24*, 48−57.

(17) Li, X.; Li, X. D. Chemical Proteomics Approaches to Examine Novel Histone Posttranslational Modifications. *Curr. Opin Chem. Biol.* **2015**, *24*, 80−90.

(18) Lai, S.; Chen, Y.; Yang, F.; Xiao, W.; Liu, Y.; Wang, C. Quantitative Site-Specific Chemoproteomic Profiling of Protein Lipoylation. *J. Am. Chem. Soc.* **2022**, *144* (23), 10320−10329.

(19) Tsushima, M.; Sato, S.; Miura, K.; Niwa, T.; Taguchi, H.; Nakamura, H. Intracellular Photocatalytic-Proximity Labeling for Profiling Protein−Protein Interactions in Microenvironments. *Chem. Commun.* **2022**, *58* (12), 1926−1929.

(20) Tamura, T.; Takato, M.; Shiono, K.; Hamachi, I. Development of a Photoactivatable Proximity Labeling Method for the Identification of Nuclear Proteins. *Chem. Lett.* **2020**, *49* (2), 145−148.

(21) Al-Nu'airat, J.; Altarawneh, M.; Gao, X.; Westmoreland, P. R.; Dlugogorski, B. Z. Reaction of Aniline with Singlet Oxygen ($O_2{}^1\Delta_g$). *J. Phys. Chem.* **2017**, *121* (17), 3199−3206.

(22) Briviba, K.; Devasagayam, T. P. A.; Sies, H.; Steenken, S. Selective Para-Hydroxylation of Phenol and Aniline by Singlet Molecular Oxygen. *Chem. Res. Toxicol.* **1993**, *6* (4), 548−553.

(23) Yang, Y.; Verhelst, S. H. L. Cleavable Trifunctional Biotin Reagents for Protein Labelling, Capture and Release. *Chem. Commun.* **2013**, *49* (47), 5366−5368.

(24) Wong, J. W. H.; Cagney, G. Proteome Bioinformatics. *Methods Mol. Biol.* **2010**, *604*, 273−283.

(25) Yamakoshi, H.; Dodo, K.; Okada, M.; Ando, J.; Palonpon, A.; Fujita, K.; Kawata, S.; Sodeoka, M. Imaging of EdU, an Alkyne-Tagged Cell Proliferation Probe, by Raman Microscopy. *J. Am. Chem. Soc.* **2011**, *133* (16), 6102−6105.

(26) Yamakoshi, H.; Dodo, K.; Palonpon, A.; Ando, J.; Fujita, K.; Kawata, S.; Sodeoka, M. Alkyne-Tag Raman Imaging for Visualization of Mobile Small Molecules in Live Cells. *J. Am. Chem. Soc.* **2012**, *134* (51), 20681−20689.

(27) Shen, X.; Hong, M.-S.; Moss, J.; Vaughan, M. BIG1, a Brefeldin A-Inhibited Guanine Nucleotide-Exchange Protein, Is Required for Correct Glycosylation and Function of Integrin B1. *Proc. National Acad. Sci.* **2007**, *104* (4), 1230−1235.

(28) Kechagia, J. Z.; Ivaska, J.; Roca-Cusachs, P. Integrins as Biomechanical Sensors of the Microenvironment. *Nat. Rev. Mol. Cell Bio* **2019**, *20* (8), 457−473.

(29) Frame, M. C.; Patel, H.; Serrels, B.; Lietha, D.; Eck, M. J. The FERM Domain: Organizing the Structure and Function of FAK. *Nat. Rev. Mol. Cell Bio* **2010**, *11* (11), 802−814.

(30) Su, Y.; Xia, W.; Li, J.; Walz, T.; Humphries, M. J.; Vestweber, D.; Cabañas, C.; Lu, C.; Springer, T. A. Relating Conformation to Function in Integrin A5β1. *Proc. National Acad. Sci.* **2016**, *113* (27), E3872−E3881.

(31) Calderwood, D. A.; Zent, R.; Grant, R.; Rees, D. J. G.; Hynes, R. O.; Ginsberg, M. H. The Talin Head Domain Binds to Integrin β Subunit Cytoplasmic Tails and Regulates Integrin Activation. *J. Biol. Chem.* **1999**, *274* (40), 28071−28074.

(32) Klapholz, B.; Brown, N. H. Talin − the Master of Integrin Adhesions. *J. Cell Sci.* **2017**, *130* (15), 2435−2446.

(33) Ivanov, I. V.; Mappes, T.; Schaupp, P.; Lappe, C.; Wahl, S. Ultraviolet Radiation Oxidative Stress Affects Eye Health. *J. Biophotonics* **2018**, *11* (7), No. e201700377.

(34) Jurkunas, U. V.; Bitar, M. S.; Funaki, T.; Azizi, B. Evidence of Oxidative Stress in the Pathogenesis of Fuchs Endothelial Corneal Dystrophy. *Am. J. Pathol.* **2010**, *177* (5), 2278−2289.
(35) McKay, T. B.; Schlötzer-Schrehardt, U.; Pal-Ghosh, S.; Stepp, M. A. Integrin: Basement Membrane Adhesion by Corneal Epithelial and Endothelial Cells. *Exp. Eye Res.* **2020**, *198*, 108138.
(36) Okumura, N.; Kakutani, K.; Numata, R.; Nakahara, M.; Schlötzer-Schrehardt, U.; Kruse, F.; Kinoshita, S.; Koizumi, N. Laminin-511 and −521 Enable Efficient In Vitro Expansion of Human Corneal Endothelial Cells. *Investigative Opthalmology Vis Sci.* **2015**, *56* (5), 2933.
(37) Parapuram, S. K.; Huh, K.; Liu, S.; Leask, A. Integrin B1 Is Necessary for the Maintenance of Corneal Structural Integrity. *Investigative Opthalmology Vis Sci.* **2011**, *52* (11), 7799.
(38) Simirskii, V. N.; Wang, Y.; Duncan, M. K. Conditional Deletion of B1-Integrin from the Developing Lens Leads to Loss of the Lens Epithelial Phenotype. *Dev. Biol.* **2007**, *306* (2), 658−668.

https://doi.org/10.1021/jacs.2c07180
J. Am. Chem. Soc. 2022, 144, 20171−20176

Supporting Information

Chemoproteomic Identification of Blue-Light-Damaged Proteins

Kohei Toh,[1] Kosuke Nishio,[1] Reiko Nakagawa,[2] Syusuke Egoshi,[3,4] Masahiro Abo,[1] Amelie Perron,[1,5] Shin-ichi Sato,[1] Naoki Okumura,[6] Noriko Koizumi,[6] Kosuke Dodo,[3,4] Mikiko Sodeoka,[3,4] Motonari Uesugi*[1,5,7]

[1]*Institute for Chemical Research, Kyoto University, Uji, Kyoto 611-0011, Japan*

[2]*Laboratory for Cell-Free Protein Synthesis, RIKEN Center for Biosystems Dynamics Research, Kobe, Hyogo 650-0047, Japan*

[3]*Synthetic Organic Chemistry Laboratory, RIKEN Cluster for Pioneering Research, 2-1 Hirosawa, Wako, Saitama 351-0198, Japan*

[4]*Catalysis and Integrated Research Group, RIKEN Center for Sustainable Resource Science, 2-1, Hirosawa, Wako, Saitama 351-0198, Japan*

[5]*Institute for Integrated Cell-Material Sciences (WPI-iCeMS), Kyoto University, Uji, Kyoto 611-0011, Japan*

[6]*Department of Biomedical Engineering, Faculty of Life and Medical Sciences, Doshisha University, Kyotanabe, Kyoto 610-0321, Japan*

[7]*School of Pharmacy, Fudan University, Shanghai 201203, China*

Table of Contents:

1. Experimental procedures

(1) Cell culture

HeLa, B16F10 and iHCEC cells were maintained in Dulbecco's Modified Eagle Medium (DMEM, #11995-065 Gibco®), supplemented with 100 units/mL penicillin (Nacalai Tesque), 100 μg/mL streptomycin sulfate (Nacalai Tesque), and 10% (v/v) fetal bovine serum (FBS, Biowest, S1820-500) at 37ºC in a humidified 5% CO_2 incubator.

(2) Materials

Chemical reagents were purchased from Sigma Aldrich, Wako, TCI, Enamine, and Click Chemistry Tools. All probes are commercially available (probe **1** (TCI, P0911); probe **2** (Enamine, EN300-705939); probe **3** (BLD pharm, BD248153); probe **4** (Wako, 351-38191); probe **5** (TCI, D2794)). All antibodies are listed below.

Antibody list		
Antibody name	**Supplier**	**Code**
GAPDH	Santa Cruz	SC-25778
ITGB1	abcam	ab52971
ITGB1	abcam	ab30394; 12G10
FAK	Cell Signaling Technology	13009
Phospho-FAK	BD Transduction	611807
c-Myc	Nacalai Tesque	04362-34
c-Myc Agarose Conjugate	Nacalai Tesque	04145-55
Anti-rabbit IgG, HRP-linked	Cell Signaling Technology	7074
Anti-mouse IgG, HRP-linked	Cell Signaling Technology	7076

(3) Plasmid amplification

Escherichia coli Competent Quick DH5α competent cells (TOYOBO) were stored at –80ºC and thawed on ice just before the transformation. The bacterial cells were grown in LB (Lennox, Nacalai Tesque) growth media at 37ºC.

(4) Plasmid construction

Total RNA from cultured HeLa cells was prepared using ISOGEN (NIPPON GENE) according to the manufacturer's protocol. cDNAs were then synthesized using PrimeScript 1st strand cDNA Synthesis Kit (Takara Bio) according to the manufacturer's protocol. The resulting cDNAs were PCR-amplified with forward and reverse primers shown below. ITGB1 gene was subcloned into the Xho I site of the pCMV_3Tag9 vector (Agilent technology) using Infusion® HD Cloning Kit

(Takara Bio). The PCR amplified sequence was verified by DNA sequencing.

Primers for ITGB1		
ITGB1	Forward	TACCGTCGACCTCGAG ATGAATTTACAACCAATTTTCTG
	Reverse	GTTTCTGCTCCTCGAG TTTTCCCTCATACTTCGGATTG

2. Method

(1) *In vitro* BSA labeling and in-gel fluorescence imaging

For *in vitro* BSA labeling, Flavin derivatives (1 μM) were used as the flavin concentration in DMEM is 1 μM. 1 mg/mL of melanin (DNP), which is comparable with the epidermal melanin concentration, was used.[1] To 8 μL of BSA solution (2 μg/μL), 10 μL of DNP (2 mg/mL stock in Milli-Q water) or 10 μL Flavin or Porphyrin derivatives (2 μM in Milli-Q water), and 2 μL of probe **1** (20 mM stock in Milli-Q water) were added. The mixture was irradiated for the indicated periods by blue light (450 nm) with an LED illumination array for 96-well plates (LEDA-450, Amuza Teleopto) equipped with a LAD driver in constant mode (LAD-1, Amuza Teleopto). The light intensity was set to 14 mW by using a light power meter (LPM-100, Amuza Teleopto). 4 volumes of ice-cold 100% methanol were added to the mixture and precipitated at –80ºC for 1 h. The mixture was centrifuged at 4ºC at 20,000 g for 20 min. The protein pellets were washed twice with 1 mL of ice-cold 100% methanol. Methanol was removed, and the protein pellets were air-dried at room temperature for LC-MS/MS analysis or fluorescence imaging. For fluorescence imaging, the pellets were resuspended with RIPA buffer (Nacalai Tesque). Click chemistry was performed by the addition of 100 μM $CuSO_4$, 200 μM THPTA ligand (3 [tris(3-hydroxypropyltriazolylmethyl)amine), 500 μM sodium ascorbate, and 50 μM TAMRA azide as final concentrations. Samples were allowed to react at room temperature for 3 h. The reaction was stopped by adding 6×SDS-PAGE reducing loading buffer (Nacalai Tesque). The proteins were resolved in a 12% SDS-PAGE acrylamide gel, and fluorescence imaging was obtained using Typhoon™ FLA 900.

(2) *In vitro* protein labeling and in-gel fluorescence imaging

To 98 μL of HeLa cell lysates (1 mg/mL), 1 μL of probes (200 mM stock in Milli-Q water), 1 μL FMN (100 μM in Milli-Q water) were added. The mixture was irradiated by blue light for 10 min (14 mW, 450 nm). To remove unreacted reagents, the reaction mixture was desalted by G-25 Columns (GE Healthcare) at 735 g for 2 min. Click chemistry was performed by the addition of 100 μM $CuSO_4$, 200 μM THPTA ligand, 500 μM sodium ascorbate, and 50 μM TAMRA azide as final concentrations in the eluted solution. Samples were allowed to react at room temperature for 3 h. The reaction was stopped by adding 6×SDS-PAGE reducing loading buffer. The proteins

were resolved in a 12% SDS-PAGE acrylamide gel, and fluorescence imaging was obtained using Typhoon™ FLA 900.

(3) Protein labeling in non-pigment cells

HeLa or iHCEC cells (2×10^6 cells) were seeded on 10-cm dishes in complete DMEM for 24 h at 37ºC. The cells were washed twice with serum-free DMEM, and incubated in medium containing probe **1** (2 mM) for 15 min. After washing twice with EBSS buffer (#24010-043, Gibco®), the cells were treated with probe **1** (2 mM) in EBSS buffer for 10 min at 37ºC. Cells were then illuminated by blue light (450 nm, 14 mW) for 10 min. Next, cells were washed once with ice-cold PBS (pH 7.4, #10010-023, Gibco®) and lysed by sonication in RIPA buffer containing 1% protease inhibitor cocktail (Nacalai Tesque). The protein concentration in each lysate was determined by a BCA protein assay kit (Thermo Scientific).

(4) Protein labeling in B16F10 cells

B16F10 cells (2×10^6 cells) were seeded on 10-cm dishes in complete DMEM for 12 h at 37ºC. For the preparation of high pigment cells, α-MSH (200 nM) was added to dishes, and the cells were incubated for 72 h. The cells were washed once with PBS, harvested, and cultured again at 2×10^6 cells per 10-cm dishes in DMEM for 24 h at 37ºC. The cells were washed twice with serum-free DMEM and treated with probe **1** (2 mM) in serum-free DMEM for 15 min at 37ºC. After washing twice with EBSS buffer, the cells were treated with probe **1** (2 mM) in EBSS buffer, and illuminated by blue light (450 nm, 14 mW) for 10 min at 37ºC. Cells were washed once with ice-cold PBS and lysed by sonication in RIPA buffer containing 1% protease inhibitor cocktail. The lysates were centrifuged at 20,000 g for 20 min, and the protein concentration in each lysate was determined by a BCA protein assay kit.

(5) Fluorescence imaging of labeled proteins

Click chemistry was performed by adding 100 μM $CuSO_4$, 200 μM THPTA ligand, 500 μM sodium ascorbate, and 50 μM TAMRA azide as final concentrations to cell lysates. Samples were allowed to react at room temperature for 3 h, and the reaction was stopped by adding 6×SDS-PAGE reducing loading buffer. The proteins were resolved in a 10–12% SDS-PAGE acrylamide gel, and fluorescence imaging was obtained using Typhoon™ FLA 900.

(6) Preparation of samples for LC-MS/MS analysis

Click chemistry was performed by adding 100 μM $CuSO_4$, 200 μM THPTA ligand, 500 μM sodium ascorbate, and 50 μM Dde biotin azide as final concentrations to cell lysates. Samples were allowed to react at room temperature for 3 h. After the reaction, 4 volumes of ice-cold MeOH,

1 volume of $CHCl_3$, and 3 volumes of H_2O were added to the reaction mixture respectively to precipitate proteins. The samples were centrifuged at 15,000 g for 20 min, and washed with ice-cold MeOH. The pellets were solubilized in PBS containing 1.2% SDS via sonication. The probe-labeled proteome samples were diluted to 0.2% SDS with 5 mL of PBS and incubated with 100 μL of streptavidin-agarose beads (Pierce™ Streptavidin Agarose, Thermo Scientific) overnight at 4ºC. The beads were washed with 5 mL 0.2 % SDS/PBS, 3×5 mL PBS, and 3×5 mL water. The beads were pelleted by centrifugation (1500×g, 3 min) between washes. The washed beads were resuspended in elution buffer (100 mM sodium phosphate + 2%(v/v) hydrazine), incubated at room temperature for 90 min with agitation, and collected by centrifugation (1400×g, 3 min).

(7) LC-MS/MS proteomics and GO enrichment analysis

For the proteins in each gel slice, peptides were extracted by the in-gel digestion protocol as described previously.[2] For the protein solutions, the SP3 method was performed to prepare the peptides for mass spectrometry analysis.[3] Mass spectra were obtained on an LTQ-Orbitrap Velos Pro (Thermo Fisher Scientific) coupled to a nanoflow UHPLC system (ADVANCE UHPLC; AMR Inc.) with Advanced Captive Spray SOURCE (AMR Inc.). The enriched peptides mixtures were loaded onto a C18 ID 0.1 mm x 20 mm, 5 μm (particle size) trap column (Acclaim PepMap 100 C18, Thermo Fisher Scientific) and then fractionated by C18, ID 0.075 × 150 mm, 3 μm (particle size) column (CELI). The peptides from in-gel digestion and SP3 were eluted at a flow rate of 300 nL/min with a linear gradient of 5–35% solvent B over 46 min and 160 min, respectively. The solvent composition of Buffer A and B is 100% H_2O, 0.1% Formic acid and 100% Acetonitrile, respectively. The mass spectrometer was programmed to carry out thirteen successive scans consisting of, first, a full-scan MS over the range 350–1,600 m/z by orbitrap at 60,000 resolution, and second and thirteenth, automatic data-dependent MS/MS scans of the twelve most intense ion signals in the first precursor scan by ion-trap detectors. MS/MS spectra were obtained by setting a normalized collision energy of 35% CID using a 2 m/z isolation width and exclusion time of 90 s for molecules of the same m/z value range. The raw data files were searched against the Homo sapiens dataset (Uniprot Proteome UP000005640, 2022_01 downloaded) with the common Repository of Adventitious Proteins (cRAP, ftp://ftp.thegpm.org/fasta/cRAP) and streptavidin sequence to recognize the contaminant proteins, using Proteome Discoverer 2.5 software (Thermo Fisher Scientific) with MASCOT ver.2.6 search engine with a false discovery rate (FDR) set at 0.01. The number of missed cleavage sites was set as 2. Carbamidomethylation of cysteine was set as a fixed modification, and Met (+O), Cys (+O), Cys ($+O_2$), Cys ($+O_3$), His (+O), His ($+O_2$), His ($+C_3H_3NO$), Tyr (+O), Tyr ($+O_2$), Tyr ($+C_3H_5NO_2$), Trp ($+O_2$), and deamination of Asn and Gln were set as variable modifications. Label-free quantification of proteins was also performed using Proteome discoverer 2.5. The parameters

were as follows: Peptides to Use: Unique + Razor, Consider Protein Groups for Peptide Uniqueness: True, Use Shared Quan Results: True, Reject Quan Results with Missing Channels: False, Precursor Abundance Based On: Intensity, Min. #Replicate Features [%]: 0, Normalization Mode: None, Scaling Mode: On All Average, Protein Abundance Calculation: Summed Abundances, N for Top N: 3, Protein Ratio Calculation: Pairwise Ratio Based, Maximum Allowed Fold Change: 100, Imputation Mode: None, Hypothesis Test: *t*-test (Background Based). Highly oxidized proteins (HOPs, $\log_2$[Light/Dark] > 2.5, p value < 0.01) were used for GO enrichment analysis by DAVID. For DAVID functional annotation clustering (biological process) of HOPs, classification stringency was set at "Medium". For oxidation site identification of ITGB1, peptide identifications were accepted if they contained a peptide threshold less than 10% FDR. To compare ion intensities of peptides with oxidized His and Tyr between the light and dark samples, the peptides that exhibited the lowest q (or $q < 0.01$) and PEP value were used.

(8) Immunostaining of ITGB1

HeLa cells (6.0×10^3 cells) were seeded on a 96-well plate and incubated for 24 h at 37ºC. The cells were washed with EBSS buffer and irradiated with blue light (450 nm, 14 mW) for 10 min at 37ºC, or treated with H_2O_2 (1 mM) for 10 min at 37ºC. After treatment, the cells were washed with ice-cold PBS and fixed with a 4% (w/v) paraformaldehyde PBS solution (Nakalai) at room temperature for 10 min. Next, cells were permeabilized with 0.1% Triton X-100 for 15 min at room temperature, followed by blocking with 0.5% (w/v) BSA/PBS at room temperature for 1 h. The resulting samples were incubated with the primary antibody (anti-active ITGB1 antibody, 12G10) at 4ºC for 3 h, and washed three times with 0.05% PBS-T (containing 0.05% (v/v) Tween 20). The samples were exposed to the secondary antibody (Alexa488 conjugated anti-mouse IgG) for 1 h at room temperature and washed three times with 0.05% PBS-T. For nuclear staining, the samples were incubated with Hoechst 33342 (in PBS, 1 μg/mL) for 15 min and washed twice with PBS. Fluorescence imaging was performed using a CellVoyager™ CQ1 confocal microscope (Yokogawa Electrical Corporation).

(9) Cell adhesion assay

HeLa cells (4×10^5 cells) were cultured on 6-cm dishes in complete DMEM for 24 h at 37ºC. HeLa cells were washed twice with serum-free DMEM at 37ºC, and incubated in medium containing NAC (2 mM) for 60 min or NaN_3 (10 mM) for 15 min. After washing twice with EBSS buffer, the cells were then illuminated by blue light (450 nm, 14 mW) for 10 min in EBSS buffer. The cells were scraped, reseeded on Fibronectin, Collagen I, or Laminin-coated plates (BioCoat™, COI), and incubated for 1 h at 37ºC. The media was aspirated, and cells were washed with ice-cold PBS. Cells were then incubated in a crystal violet solution (Crystal violet powder: 0.125g,

in 10 mL methanol and 40 mL H_2O) for 15 min, and rinsed four times with PBS. The stained cells were then treated with a lysis solution (0.1 M sodium citrate, 25% ethanol, pH 4.2) for 30 min while shaking gently on a rocking shaker. The solution was aspirated and diluted for OD measurements at 590 nm.

(10) Analysis of ITGB1 downstream signaling

HeLa cells (4×10^5 cells) were cultured on 6-cm dishes in DMEM for 24 h at 37ºC. HeLa cells were washed twice with EBSS buffer at room temperature and illuminated with blue LED light (450 nm, 14 mW) for 10 min in EBSS buffer. The cells were scraped, reseeded on Fibronectin, Collagen I, or Laminin coated plates (BioCoat™, COI), and incubated for 1 h. Cells were then scraped again, and the pellets were obtained after centrifugation at 1000×g for 20 sec and washed with ice-cold PBS. Cell lysates were prepared by sonication and centrifugation at 20,000 g for 20 min with RIPA buffer. The concentration of the proteins in lysates was determined by a BCA protein assay kit before Western blot analysis.

(11) Western blot analysis

HeLa cell lysates or biotin pull-down samples were mixed with 6×SDS-PAGE loading buffer and boiled at 95ºC for 3 min. The proteins were separated by SDS-PAGE and transferred to a nitrocellulose membrane (Protoran™, 0.45 μm, GE Healthcare) by electroblotting. The membrane was blocked with 5% (w/v) skim milk for 1 h, washed with 0.05% PBS-T, and then incubated with primary antibodies overnight at 4ºC. After additional washing with PBS-T, membranes were probed with a horseradish peroxidase-conjugated secondary antibody at room temperature for 1 h, followed by ECLTM detection (Prime Western Blotting Detection Reagent, GE Healthcare). The bands were visualized using ImageQuant LAS 500 imaging system (GE Healthcare).

(12) Purification of 3×c-Myc ITGB1 after blue light irradiation

HeLa cells (2×10^6 cells) were seeded on 10-cm dishes in complete DMEM for 24 h at 37ºC. ITGB1 inserted pCMV_3Taq9 plasmid was transfected to HeLa cells using Lipofectamine® 3000 Reagent (Thermo Fisher). The transfected cells were incubated at 37ºC for 24 h. The cells were washed once with PBS and incubated for an additional 24 h in DMEM. After washing twice with EBSS, Cells were illuminated by blue light (450 nm, 14 mW) for 10 min at 37ºC. The cells were washed once with ice-cold PBS, harvested in ice-cold PBS, and homogenized by Dounce homogenizer. After centrifuging at 20,000 g for 20 min, the supernatant was removed, and RIPA buffer was added to the pellet. Next, samples were sonicated and centrifuged at 20,000 g for 20 min. The protein concentration from the supernatant was determined by a BCA protein assay kit,

and diluted to 2 mg/mL by RIPA buffer. The samples (1.0 mL) were mixed with 25 μL of agarose-conjugated anti-c-Myc antibody (Nacalai Tesque) by gentle rotation at 4ºC for 24 h. The beads were recovered by centrifugation at 1,500 g for 3 min washed once with RIPA buffer, and three times with PBS (1 mL). After the last washing step, the beads were boiled at 95ºC for 5 min with 2×SDS-PAGE loading buffer. The eluted proteins in the sample were separated by SDS-PAGE, and the bands of interest were cut for LC-MS/MS analysis.

(13) Synthesis of artificial melanin

As reported by Gianneschi *et al.*,[4] dopamine (50 mg) was dissolved in 25 mL of Milli-Q water and transferred to a clean round bottom flask. 63 μL of ammonium hydroxide were added to the reaction flask under vigorous stirring. The reaction was exposed to air and stirred at room temperature for 24 h. For purification, the dark brown to black melanin samples were centrifuged at 11,000 rpm for 10 min. Supernatant was collected and purified by centrifugal filtration (10 kDa, Amicon® Ultra-15), washing with Milli-Q water. Then, aggregates were removed by centrifugation at 14,000 rpm for 10 min, followed by 0.22 μm filtration. The mass concentration of the melanin solution was determined by lyophilizing a known volume of the final solution overnight and then weighing the sample.

(14) Modification of amino acids with probe 1

As reported by Nakane and Sato *et al.*,[5] Fmoc-His-OMe or Fmoc-Tyr-OMe (final conc. = 1 mM), probe **1** (final conc. = 1 mM) and FMN (final conc. = 1 mM) in 75% MeCN/PBS buffer (pH7.4) was added to a 1.5 mL tube. 100 μL of the reaction mixture was incubated at 37ºC for 5 min in the presence of blue light (450 nm, 14 mW). After the reaction, the reaction mixture was diluted by MeCN, and analyzed by HRMS (JEOL MStation MS-700V).

(15) Calculating the area ratio of propargylamine to propargylammonium ion

The 100 mM probe **1**/propargylamine hydrochloride in Milli-Q water containing 1% MeCN, as an internal standard, was placed on a 4-well glass bottom dish. The Raman spectra of each sample were measured by using a slit-scanning Raman microscope with 532 nm excitation. The measurement was repeated 4 times for each test compound. The light intensity at the sample plane was calculated as 3.0 mW/μm^2. The exposure time for each line was 10 sec. The background of water was subtracted from the measured spectra, and obtained spectra were fitted with a Gaussian function. The peak areas were calculated by "Raman viewer" software (Nanophoton Corp., Japan) equipped on the Raman microscope. Finally, the relative Raman intensity of propargylamine vs propargylammonium ion was calculated from the peak areas of alkyne of propargylamine vs MeCN and MeCN vs alkyne of propargylammonium ion.

(16) Procedures for Raman imaging in HeLa cells

HeLa cells (1.2×10^5 cells) were seeded on a sterilized Φ25 mm quartz substrate in a TPP tissue culture dish (No. 93040; TPP Techno Plastic Products AG, Switzerland) in DMEM containing 10% FBS for 24 h at 37ºC. The cells were washed twice with serum-free DMEM, and incubated in the medium containing probe **1** (0 or 2 mM) for 15 min. After washing twice with EBSS buffer, the cells were treated with probe **1** (0 or 2 mM) in EBSS buffer without phenol red for 10 min at 37°C. A quartz substrate was used to observe the Raman spectra with a slit-scanning Raman microscope at 532 nm excitation. The laser output was focused onto the sample using a 60×/1.27 numerical aperture (NA) water immersion objective lens. The slit width of the spectrograph was 50 μm. The exposure time for each line was 10 sec. The light intensity at the sample plane was calculated as 3.0 mW/μm^2. To obtain the Raman images, the Raman spectral data set was further processed using the singular value decomposition (SVD) technique for noise reduction.[6] We selected several spectral regions (700-3100 cm^{-1} for C-H bonds, 2000-2300 cm^{-1} for the C≡C bond of probe **1**) in the calculation procedure for SVD to avoid artifacts in the constructed images. A modified polyfit technique was then used at each pixel to determine the autofluorescence baseline signal, which was subtracted from the original Raman spectrum.[7] Finally, the Raman images were reconstructed using each vibrational band of interest. All data processing was performed using "Raman Viewer" image processing software.

3. Supplementary results

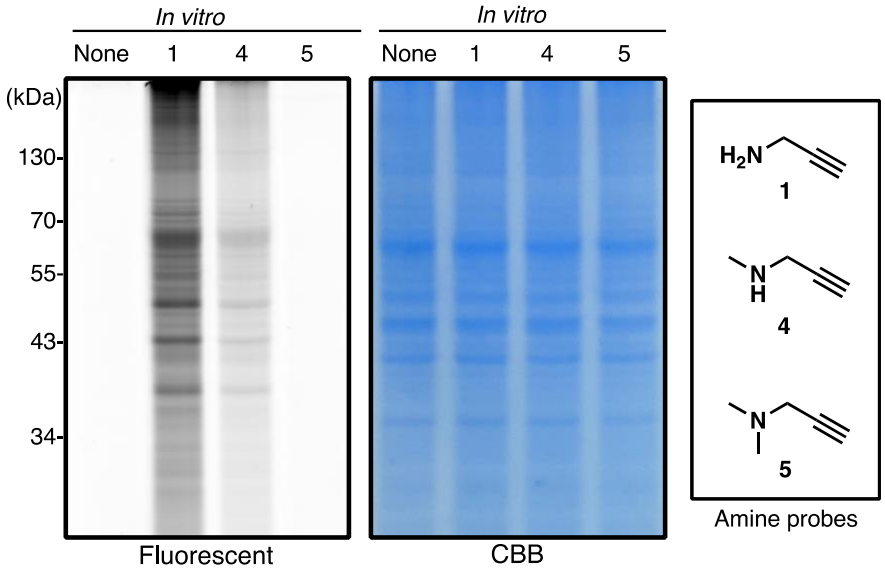

Figure S1. Comparison of primary, secondary, and tertiary amines for protein labeling. HeLa cell lysates were irradiated by blue light for 10 min with each amine probe (2 mM) and FMN (1 μM).

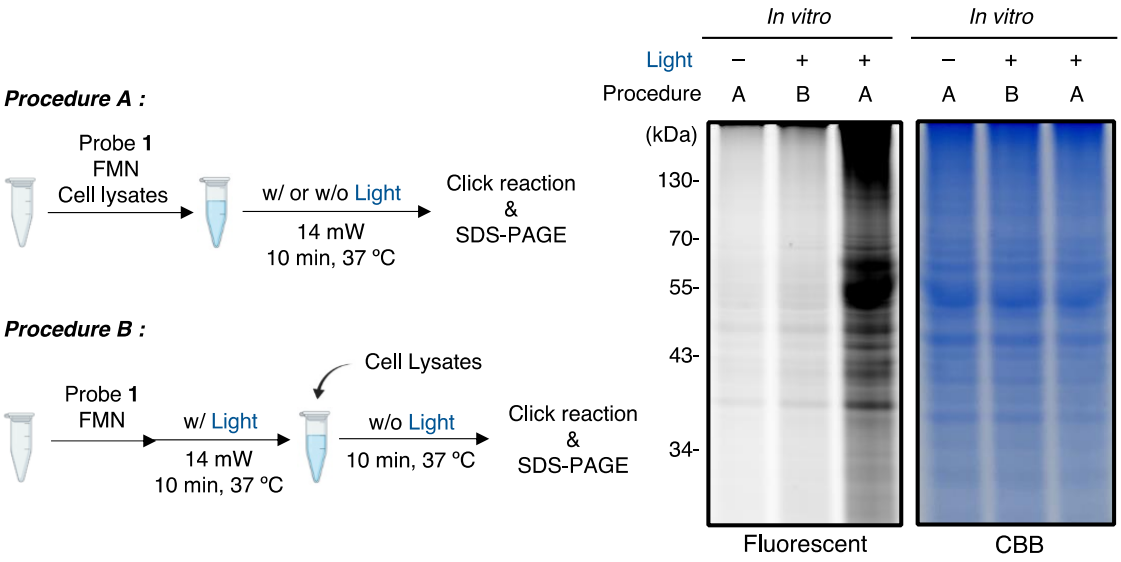

Figure S2. *In vitro* protein labeling with probe **1** under two different procedures. Procedure A: HeLa cell lysates (1 mg/mL) were irradiated by blue light for 10 min in the presence of probe **1** (2 mM) and FMN (1 μM) at 37ºC. Procedure B: After probe **1** (4 mM) in PBS was irradiated by blue light for 10 min in the presence of FMN (2 μM), the irradiated sample was added to HeLa cell lysates (final concentrations: probe **1** (2 mM); FMN (1 μM); cell lysates (1 mg/mL)) and then incubated for 10 min at 37ºC.

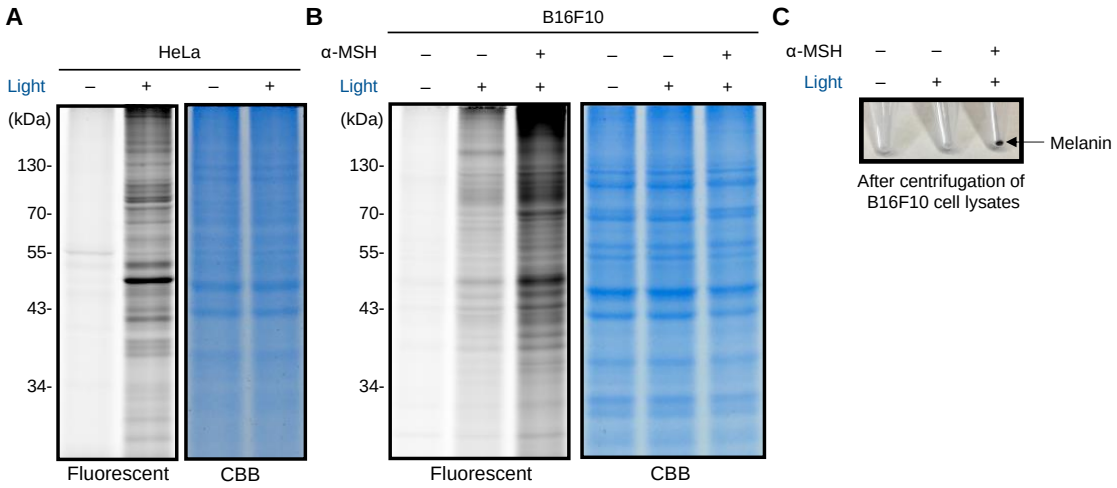

Figure S3. Fluorescent and CBB images of labeled proteins on SDS-PAGE gels. (A, B) HeLa (A) or B16F10 (B) cells were treated with probe **1** in the presence or absence of blue light irradiation. (C) Melanogenesis in B16F10 cells. Images were captured after centrifugation of B16F10 cell lysates after blue light irradiation.

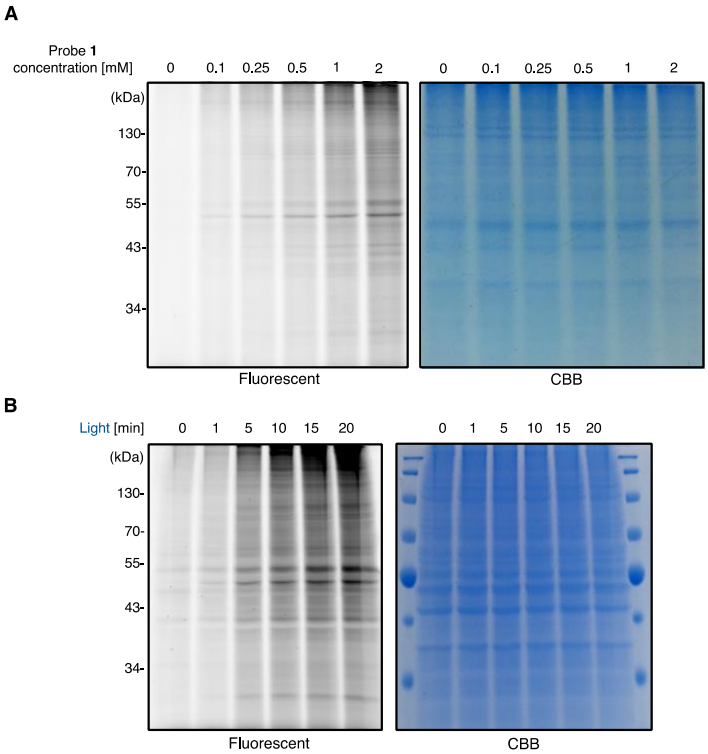

Figure S4. Concentration- and time-dependent protein labeling with probe **1**. Fluorescent and CBB images of labeled proteins on SDS-PAGE gels are shown. (A) HeLa cells were treated with different concentrations of probe **1** under blue light irradiation for 10 min. (B) HeLa cells were treated with probe **1** (2 mM) for a varied length of blue light-exposure time.

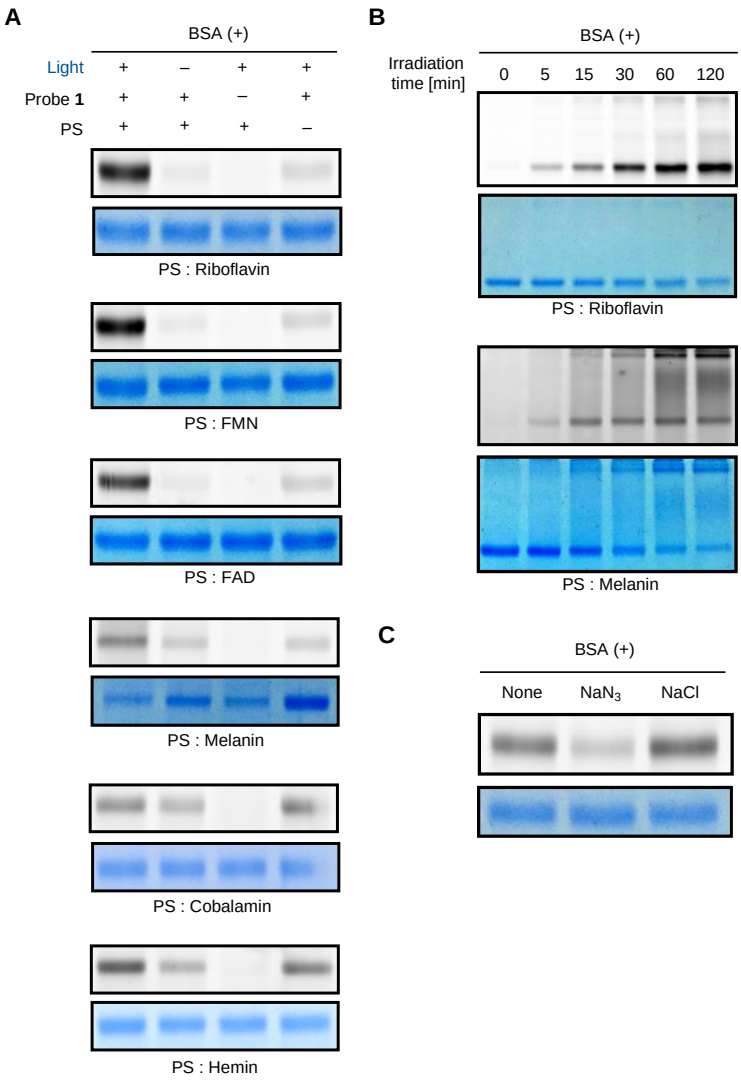

Figure S5. BSA labeling with probe **1** in the presence of photosensitizers (PS). The labeled BSA was click-reacted with TAMRA azide. The status of BSA was monitored by fluorescence scanning and CBB-staining of SDS-PAGE gels. (A) Flavin derivatives (1 μM), porphyrin derivatives (1 μM), or melanin (1 mg/mL) were used as PS. Reactions were conducted with BSA (0.8 μg/uL), probe **1** (2 mM), and PS under blue light irradiation for 15 min. (B) BSA (0.8 μg/uL) was irradiated with blue light for the indicated time in the presence of probe **1** (2 mM), and riboflavin (1 μM), or melanin (1 mg/mL). (C) BSA (0.8 μg/uL) was irradiated by blue light irradiation for 15 min in the presence of probe **1** (2 mM), riboflavin (1 μM), and different salts (10 mM).

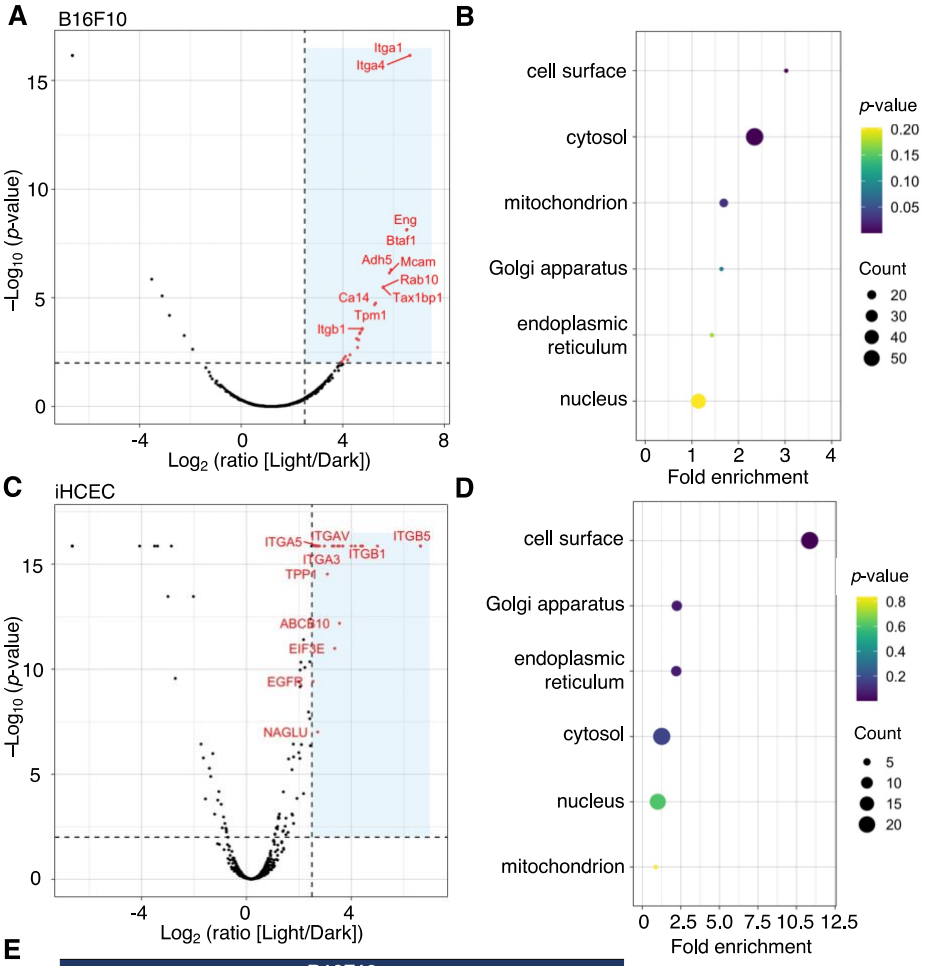

E

B16F10		
Enrichment Score: 2.01 GO Term (Biological Process)	*p* value	Fold enrichment
cell adhesion mediated by integrin	2.0.E-03	15.8
cell-matrix adhesion	3.1.E-03	8.2
integrin-mediated signaling pathway	1.5.E-01	4.4
iHCEC		
Enrichment Score: 4.90 GO Term (Biological Process)	*p* value	Fold enrichment
cell adhesion mediated by integrin	2.1.E-07	44.4
cell-substrate adhesion	2.2.E-03	42.3
endodermal cell differentiation	1.5.E-04	38.2
heterotypic cell-cell adhesion	4.2.E-03	30.6
cell-matrix adhesion	6.4.E-08	22.1
integrin-mediated signaling pathway	1.7.E-06	18.9
positive regulation of cell migration	2.2.E-05	9.3
cell adhesion	3.1.E-09	8.0
cell-cell adhesion	3.7.E-03	7.8

Figure S6. Proteomic analysis of probe **1**-labeled proteins in B16F10 and iHCEC. (A, C) Volcano plots (ratio [Light/Dark] vs *p* value) of B16F10 (A) and iHCEC (C). Highly oxidized proteins (HOPs, $\log_2$[Light/Dark] > 2.5, *p* value < 0.01) are indicated as red dots. (B, D) Subcellular localization of HOPs in B16F10 and iHCEC. GO enrichment analysis (cellular component) was conducted for the HOPs in each cell line. (E) Functional annotation clustering (biological process) of HOPs in each cell line.

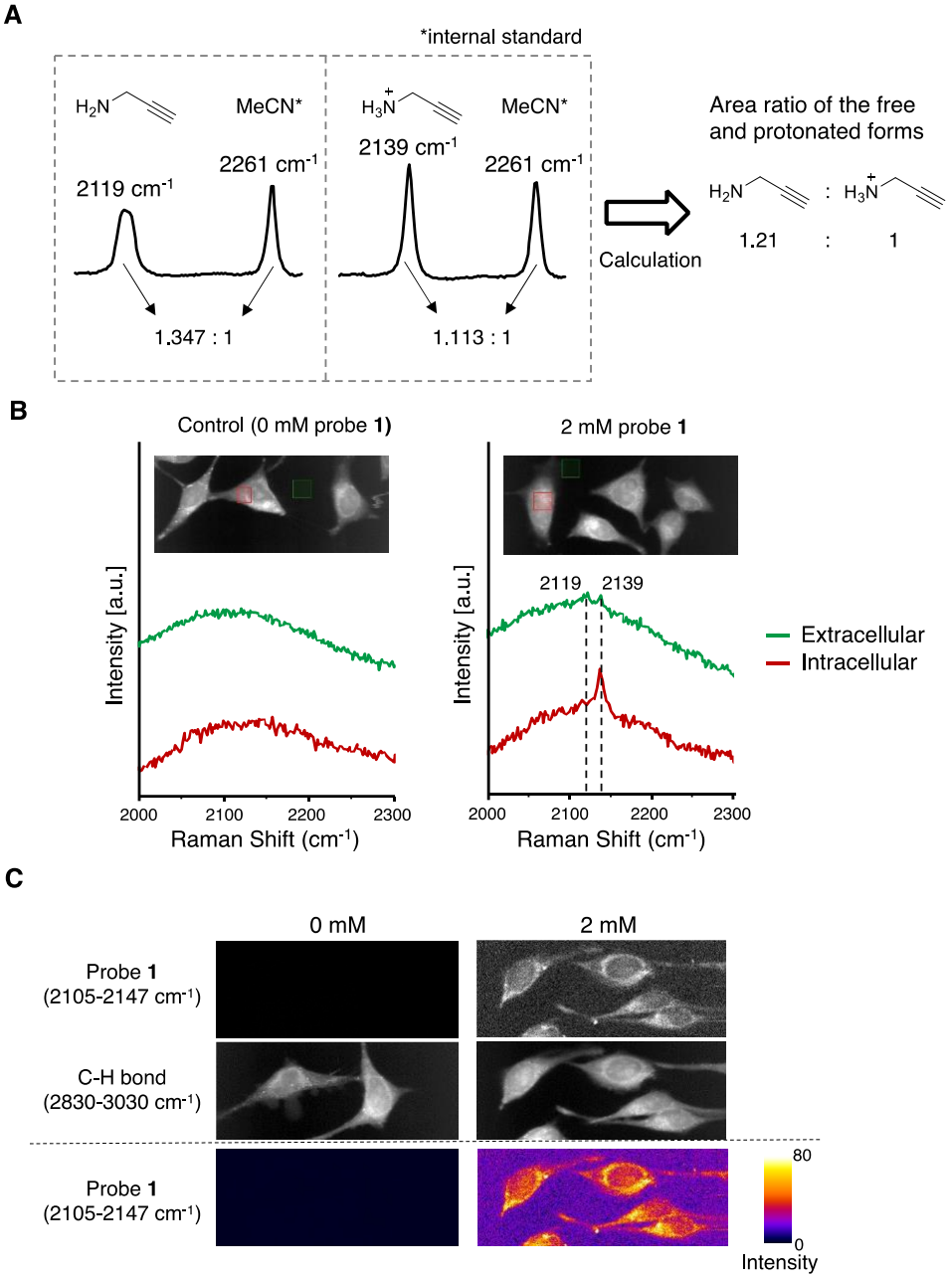

Figure S7. Detection of probe **1** by Raman microscopy. (A) Alkyne Raman signals of probe **1**. The free and protonated forms of probe **1** display slightly distinct Raman signals in water. MeCN was used as an internal standard. (B) Averaged Raman spectra of extracellular and intracellular areas in the presence (*right*) or absence (*left*) of 2 mM probe **1**. Extracellular and intracellular regions (30 × 30 pixels each) were selected for the analysis, and their corresponding Raman spectra are shown in green and red, respectively. (C) Raman imaging in HeLa cells in the presence or absence of probe **1** (2 mM). The images of probe **1** were obtained from the corrected peak areas from 2105 to 2147 cm^{-1}, while those of C-H bond were from 2830 to 3030 cm^{-1}.

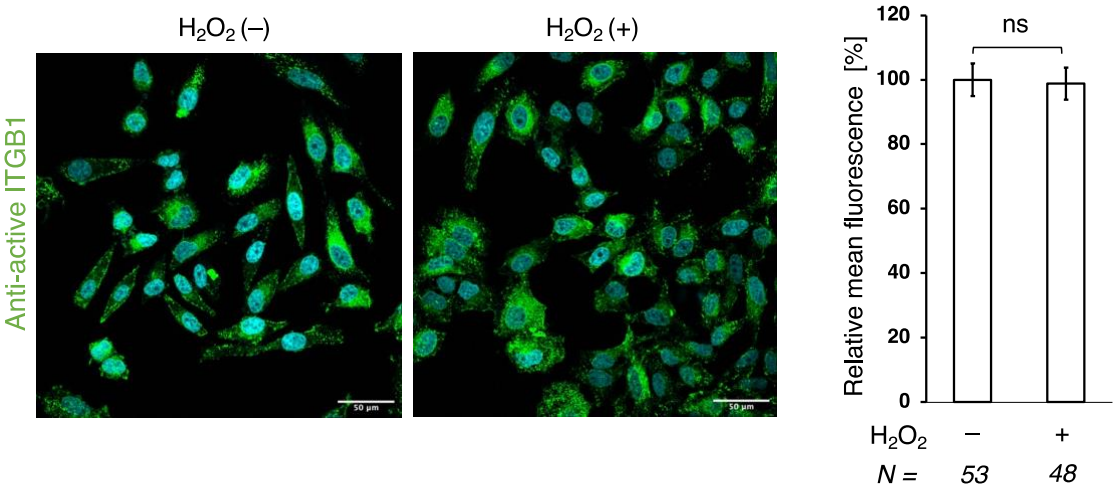

Figure S8. Immunostaining of active ITGB1 in HeLa cells in the presence of H_2O_2 (1 mM). Color code: green, active ITGB1; cyan, Hoechst 33342. The values represent the mean of fluorescence ± SD (n = 53 w/o H_2O_2; n = 48 w/ H_2O_2). Significance was determined using an unpaired two-tailed Student's t-test.

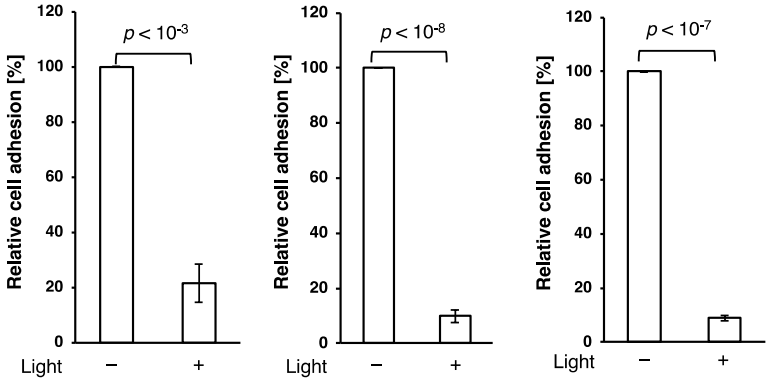

Figure S9. Effect of blue light exposure on cell adhesion. HeLa cells were reseeded onto Collagen I coated plates after 10-min blue light irradiation. Data represent averages ± SD from 3 independent experiments. Significance was determined using an unpaired two-tailed Student's t-test.

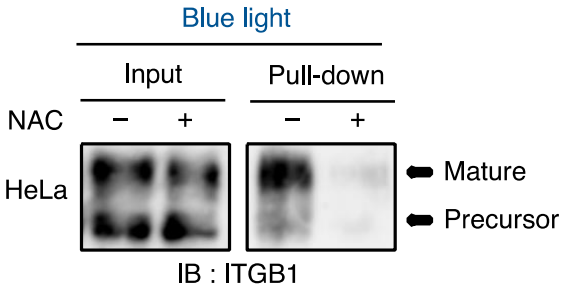

Figure S10. Pull-down and Western blot analysis of ITGB1 after blue light irradiation for 10 min with probe **1** (2 mM) in the presence or absence NAC (2 mM).

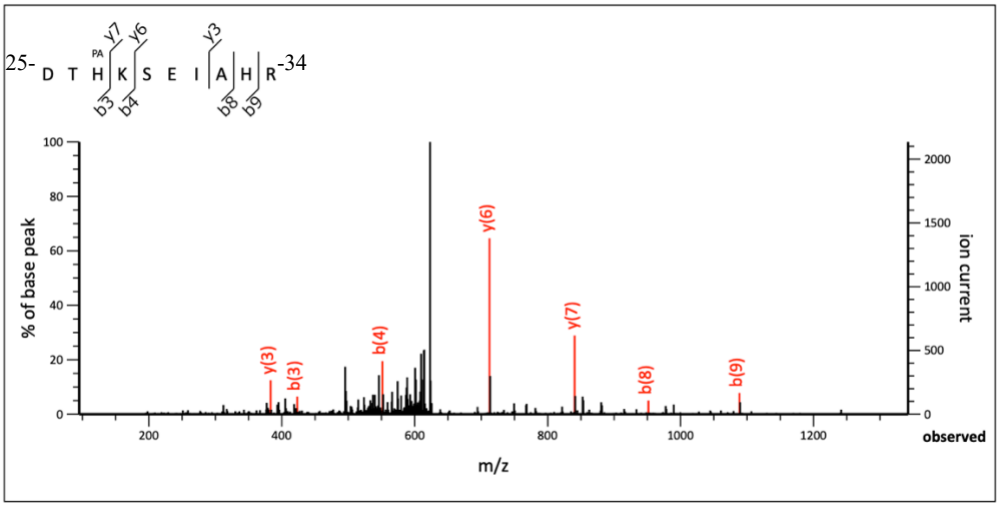
25- D T H K S E I A H R -34
PA
y7
y6
y3
b3
b4
b8
b9
% of base peak
ion current
m/z
observed
y(6)
y(7)
b(4)
y(3)
b(3)
b(8)
b(9)

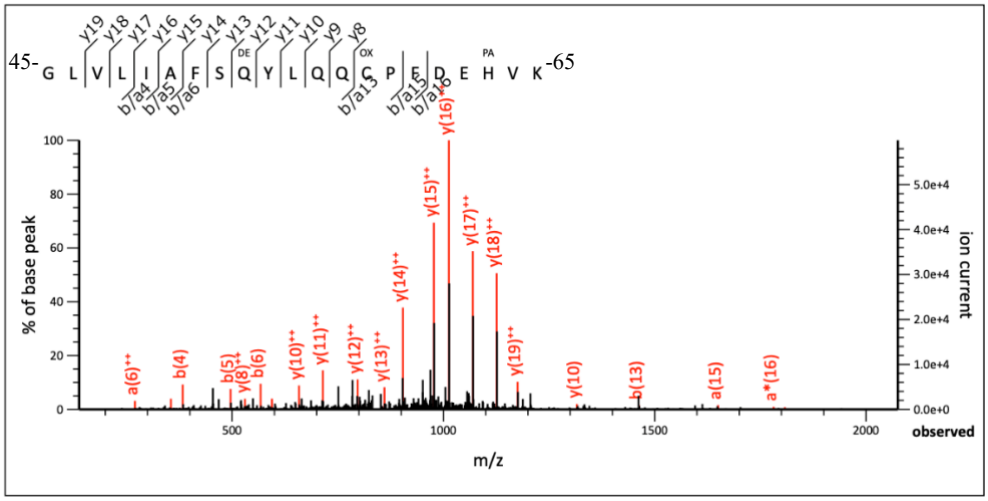
45- G L V L I A F S Q Y L Q Q C P E D E H V K -65
DE
OX
PA
% of base peak
ion current
m/z
observed
y(16)++
y(15)++
y(17)++
y(18)++
y(14)++
y(11)++
y(12)++
y(13)++
y(19)++
y(10)++
a(6)++
b(4)
b(5)
y(8)++
b(6)
y(10)
b(13)
a(15)
a*(16)

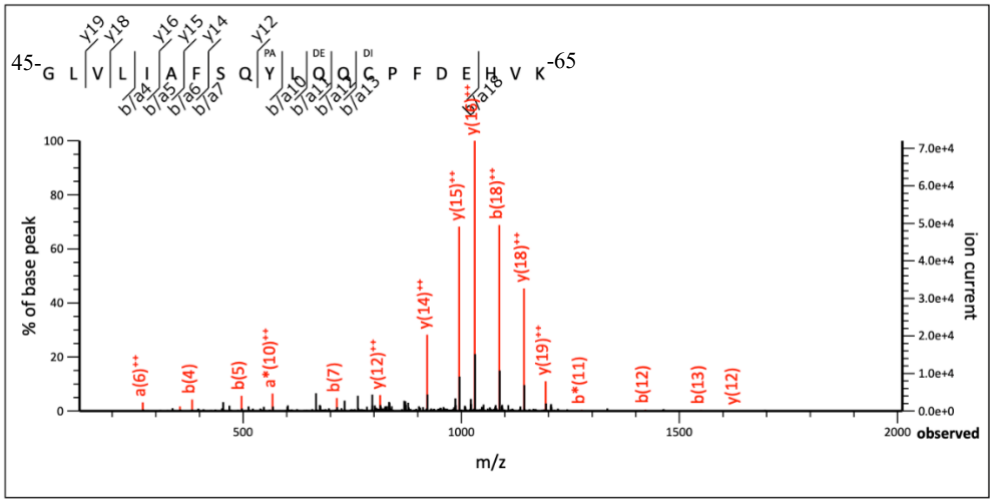
45- G L V L I A F S Q Y L Q Q C P F D E H V K -65
PA
DE
DI
% of base peak
ion current
m/z
observed
y(16)++
y(15)++
b(18)++
y(18)++
y(14)++
y(19)++
a(6)++
b(4)
b(5)
a*(10)++
b(7)
y(12)++
b*(11)
b(12)
b(13)
y(12)

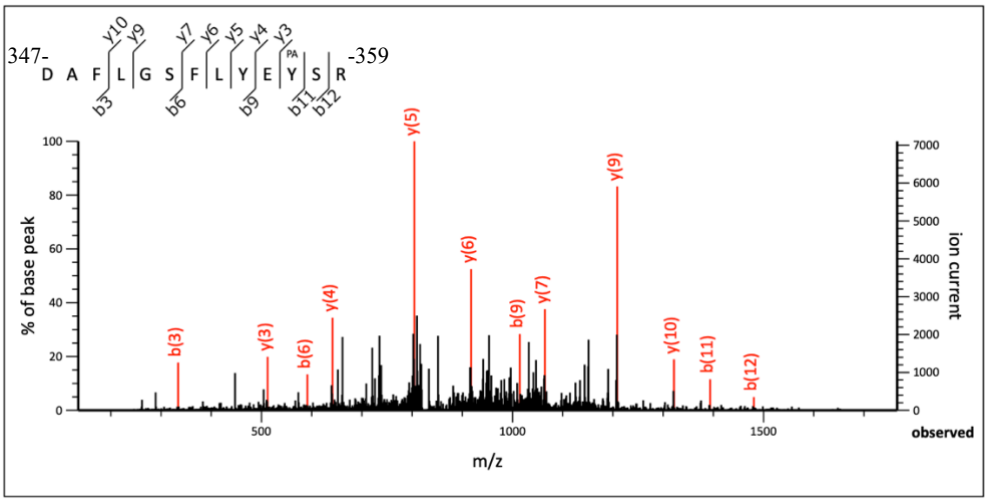

Figure S11. BSA labeling experiment with probe **1**. LC-MS/MS analysis of trypsin-digested peptide fragments of labeled BSA by MASCOT Server 2.6 (Matrix Science). MS/MS fragment assignment of labeled peptide in H27, H63, Y54, and Y357. Cys (+O = OX), Cys (+O_2 = DI), His (+C_3H_3NO = PA), Tyr (+$C_3H_5NO_2$ = PA), and deamination of Gln (DE) were included as variable modifications, while carbamidomethylation of Cys was set as a fixed modification.

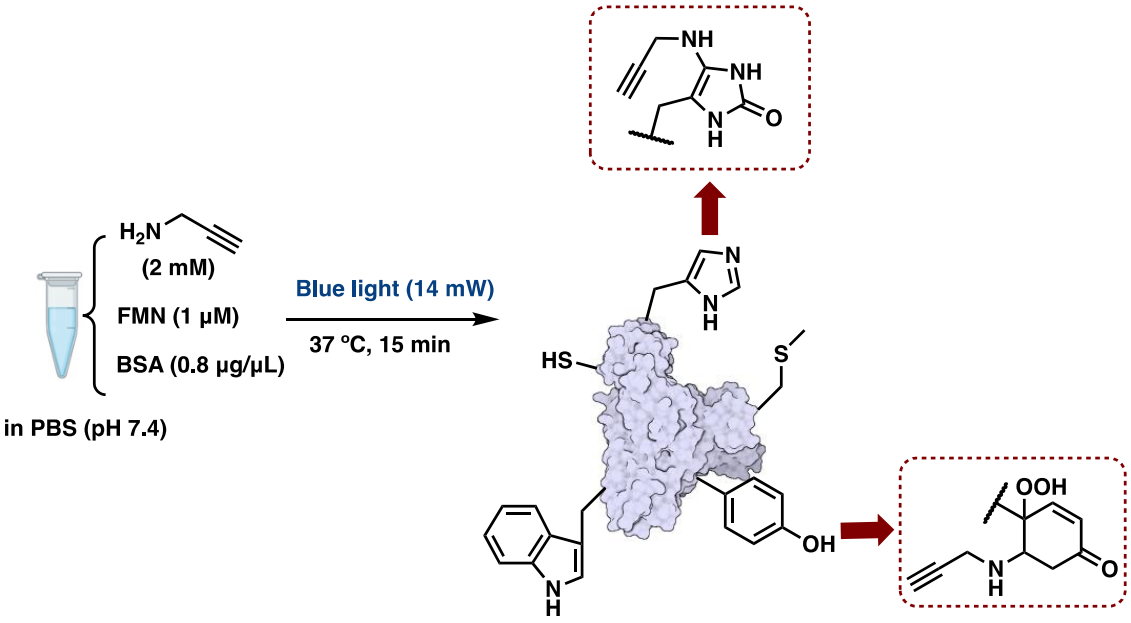

Figure S12. Proposed probe **1**-labeled amino acids in BSA.

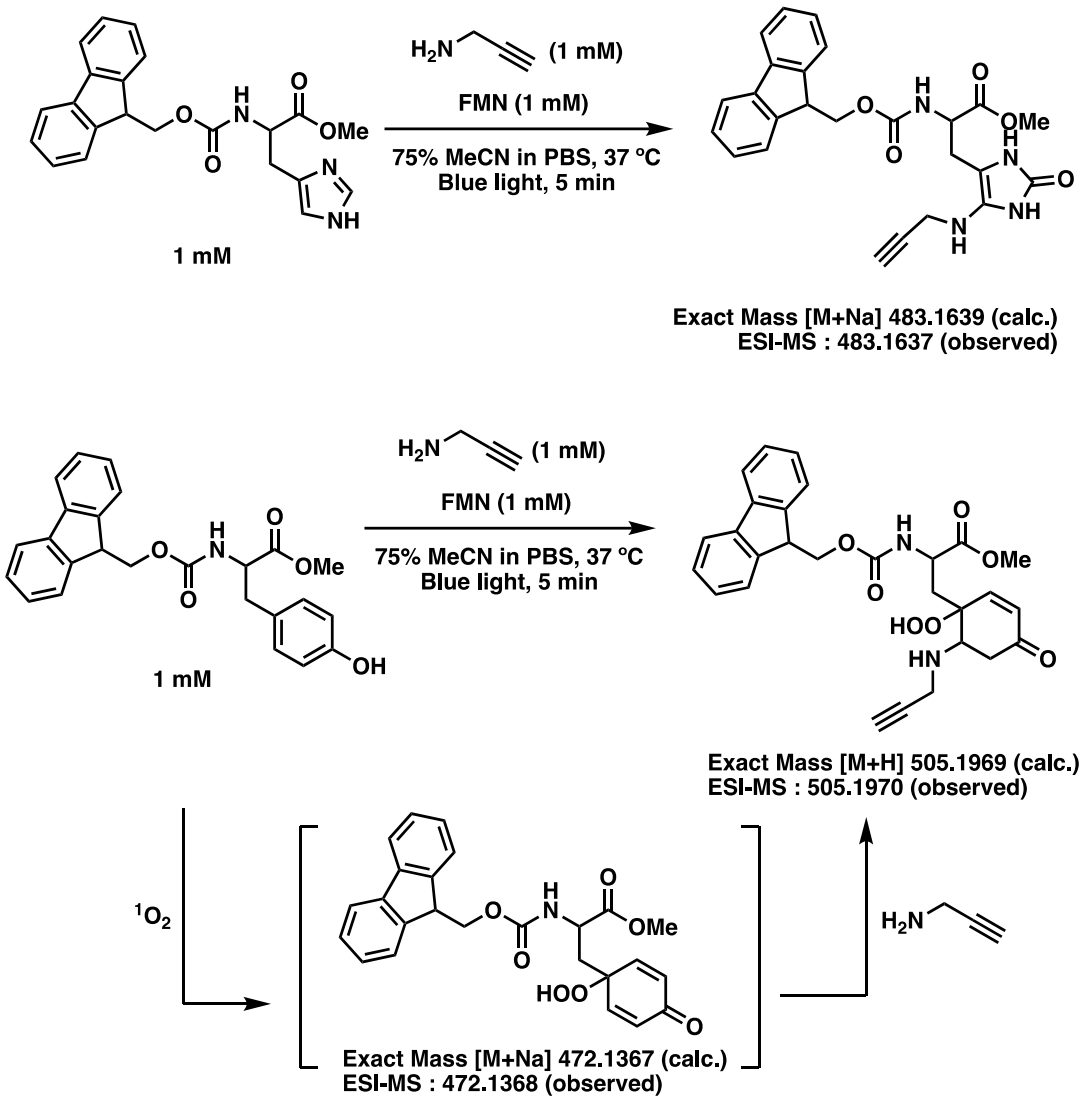

Scheme S1. Modification of amino acids with probe **1** under blue light irradiation.

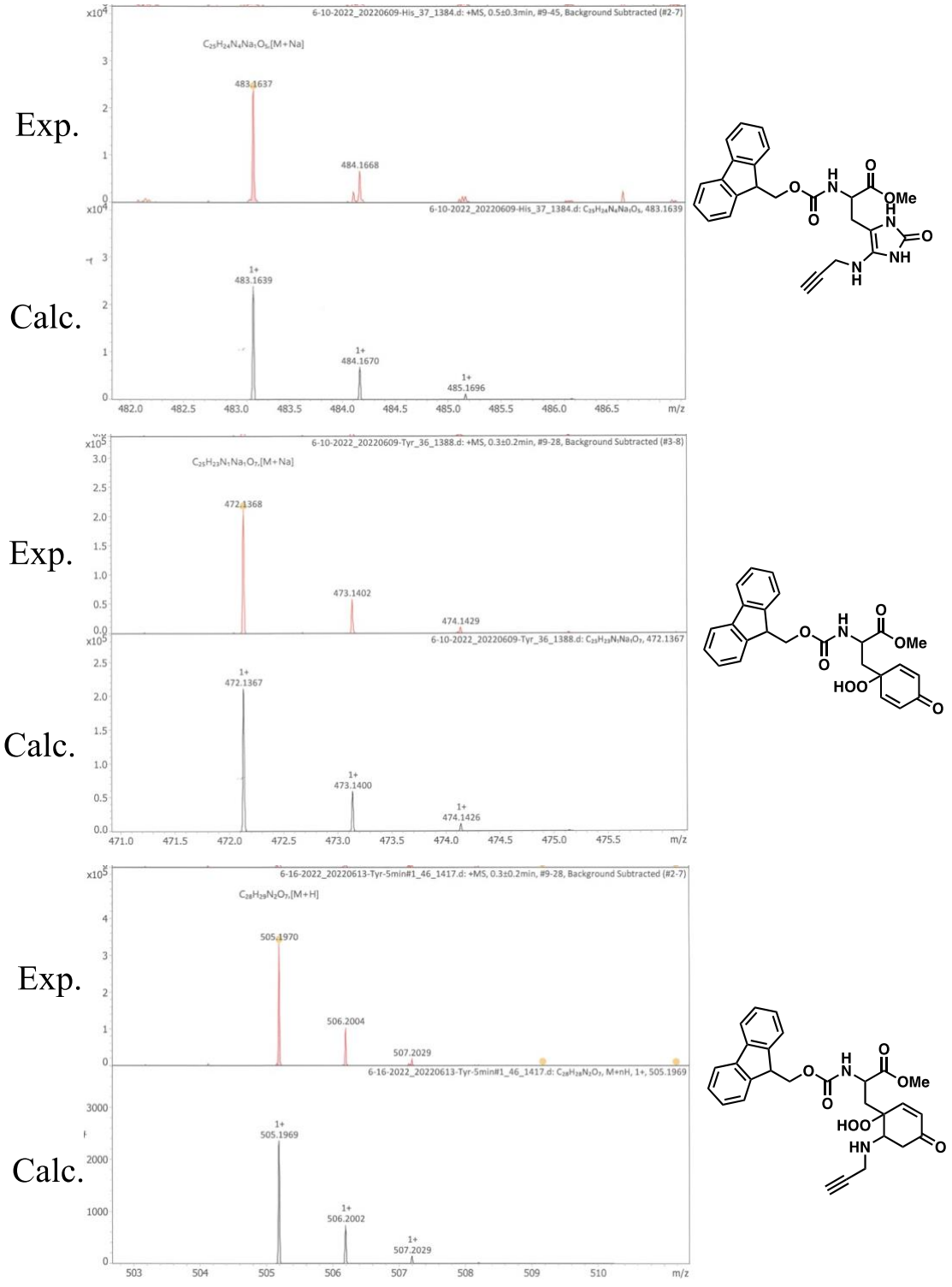

Figure S13. ESI-MS analysis of Fmoc-His and Fmoc-Tyr labeled by probe **1**.

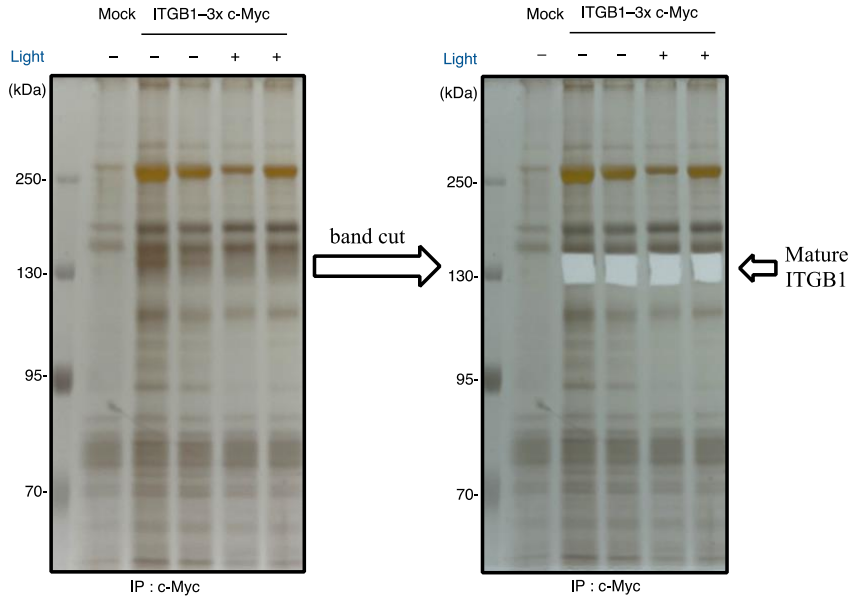

Figure S14. A silver-stained SDS-PAGE gel before and after the excision of the ITGB1 bands. HeLa cells overexpressing c-Myc-tagged ITGB1 were incubated in the presence or absence of blue-light irradiation for 10 min, and their cell lysates were prepared. c-Myc-tagged ITGB1 was immunopurified with a c-Myc antibody and separated on an SDS-PAGE gel (8%). The bands corresponding to ITGB1 were excised for LC-MS/MS analysis.

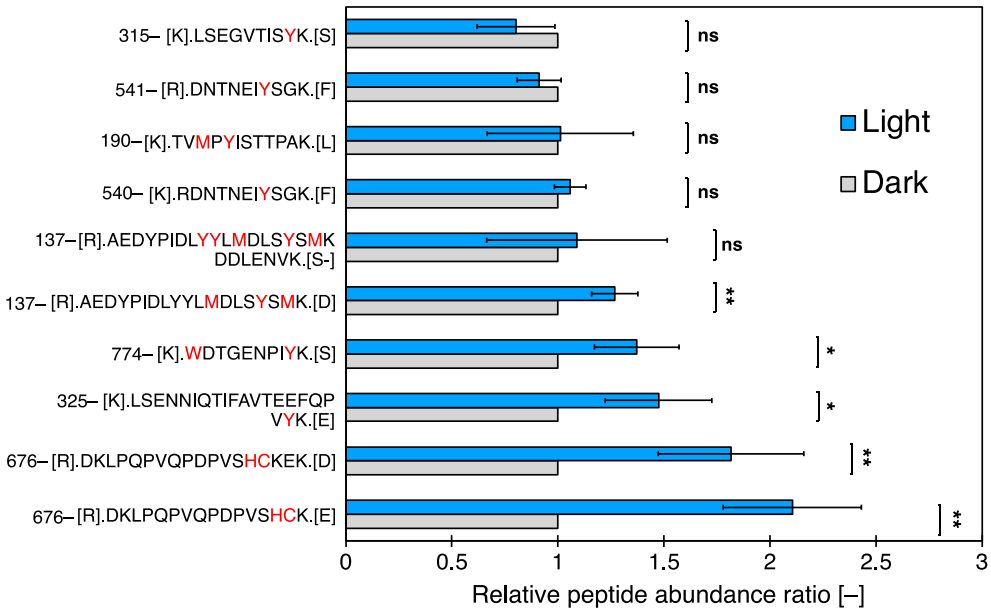

Figure S15. Detection of blue light-oxidized peptides from ITGB1. Trypsin-digested 3×c-Myc-tagged-ITGB1 peptides from untreated or blue light-exposed samples (n = 3) were analyzed by LC-MS/MS with MASCOT ver.2.6 search engine. Oxidations of Met (+O), His ($+O_2$), Tyr (+O), Tyr ($+O_2$), Trp ($+O_2$), Cys (+O), and Cys ($+O_3$) are indicated in red. Data represent average ± SD. Significance was determined using a one-sided t-test: *$p < 0.1$; **$p < 0.05$.

(A) Dark samples: Protein coverage 55 % (n = 3)

1 MNLQPIFWIG LISSVCCVFA QTDENRCLKA NAKSCGECIQ AGPNCGWCTN STFLQEGMPT 60
61 SARCDDLEAL KKKGCPPDDI ENPRGSKDIK KNKNVTNRSK GTAEKLKPED ITQIQPQQLV 120
121 LRLRSGEPQT FTLKFKRAED YPIDLYYLMD LSYSMKDDLE NVKSLGTDLM NEMRRITSDF 180
181 RIGFGSFVEK TVMPYISTTP AKLRNPCTSE QNCTSPFSYK NVLSLTNKGE VFNELVGKQR 240
241 ISGNLDSPEG GFDAIMQVAV CGSLIGWRNV TRLLVFSTDA GFHFAGDGKL GGIVLPNDGQ 300
301 CHLENNMYTM SHYYDYPSIA HLVQKLSENN IQTIFAVTEE FQPVYKELKN LIPKSAVGTL 360
361 SANSSNVIQL IIDAYNSLSS EVILENGKLS EGVTISYKSY CKNGVNGTGE NGRKCSNISI 420
421 GDEVQFEISI TSNKCPKKDS DSFKIRPLGF TEEVEVILQY ICECECQSEG IPESPKCHEG 480
481 NGTFECGACR CNEGRVGRHC ECSTDEVNSE DMDAYCRKEN SSEICSNNGE CVCGQCVCRK 540
541 RDNTNEIYSG KFCECDNFNC DRSNGLICGG NGVCKCRVCE CNPNYTGSAC DCSLDTSTCE 600
601 ASNGQICNGR GICECGVCKC TDPKFQGQTC EMCQTCLGVC AEHKECVQCR AFNKGEKKDT 660
661 CTQECSYFNI TKVESRDKLP QPVQPDPVSH CKEKDVDDCW FYFTYSVNGN NEVMVHVVEN 720
721 PECPTGPDII PIVAGVVAGI VLIGLALLLI WKLLMIIHDR REFAKFEKEK MNAKWDTGEN 780
781 PIYKSATTV VNPKYEGK

(B) Light samples: Protein coverage 56% (n = 3)

1 MNLQPIFWIG LISSVCCVFA QTDENRCLKA NAKSCGECIQ AGPNCGWCTN STFLQEGMPT 60
61 SARCDDLEAL KKKGCPPDDI ENPRGSKDIK KNKNVTNRSK GTAEKLKPED ITQIQPQQLV 120
121 LRLRSGEPQT FTLKFKRAED YPIDLYYLMD LSYSMKDDLE NVKSLGTDLM NEMRRITSDF 180
181 RIGFGSFVEK TVMPYISTTP AKLRNPCTSE QNCTSPFSYK NVLSLTNKGE VFNELVGKQR 240
241 ISGNLDSPEG GFDAIMQVAV CGSLIGWRNV TRLLVFSTDA GFHFAGDGKL GGIVLPNDGQ 300
301 CHLENNMYTM SHYYDYPSIA HLVQKLSENN IQTIFAVTEE FQPVYKELKN LIPKSAVGTL 360
361 SANSSNVIQL IIDAYNSLSS EVILENGKLS EGVTISYKSY CKNGVNGTGE NGRKCSNISI 420
421 GDEVQFEISI TSNKCPKKDS DSFKIRPLGF TEEVEVILQY ICECECQSEG IPESPKCHEG 480
481 NGTFECGACR CNEGRVGRHC ECSTDEVNSE DMDAYCRKEN SSEICSNNGE CVCGQCVCRK 540
541 RDNTNEIYSG KFCECDNFNC DRSNGLICGG NGVCKCRVCE CNPNYTGSAC DCSLDTSTCE 600
601 ASNGQICNGR GICECGVCKC TDPKFQGQTC EMCQTCLGVC AEHKECVQCR AFNKGEKKDT 660
661 CTQECSYFNI TKVESRDKLP QPVQPDPVSH CKEKDVDDCW FYFTYSVNGN NEVMVHVVEN 720
721 PECPTGPDII PIVAGVVAGI VLIGLALLLI WKLLMIIHDR REFAKFEKEK MNAKWDTGEN 780
781 PIYKSATTV VNPKYEGK

Figure S16. Integrin β1 protein sequence coverage of the Dark (A) and Light (B) samples. The peptide detected by LC-MS/MS analysis were marked in yellow, and the amino acids oxidized by blue light irradiation were indicated in red.

4. References

1. Karsten, A. E. and Smit, J. E. *Photochemistry and Photobiology*, **2012**, *88*, 469–474.
2. Oya, E.; Nakagawa, R.; Yoshimura, Y.; Tanaka, M.; Nishibuchi, G.; Machida, S.; Shirai, A.; Ekwall, K.; Kurumizawa, H.; Tagami, H. and Nakayama, J. *EMBO Reports* **2019**, *20*, e48111.
3. Hughes, C. S.; Moggridge, S.; Müller, T.; Sorensen, P. H. Morin G. B. and Krijgsveld, J. *Nat. Protc.* **2019**, *14*, 68–85.
4. Cao, W.; Mantanona, A. J.; Mao, H.; McCallum, N. C.; Jiao, Y.; Battistella, C.; Caponetti, V.; Zang, N.; Thompson, M. P.; Montalti, M.; Stoddart, J. F.; Wasielewski, M. R.; Rinehart, J. D. and Gianneschi, N. C. *Chem. Mater*. **2020**, *32*, 5759−5767.
5. Nakane, K.; Sato, S.*; Niwa, T.; Tsushim, M.; Tomoshige, S.; Taguchi, H.; Ishikawa, M. and Nakamura, M. *J. Am. Chem. Soc*. **2021**, *143*, 7726–7731.
6. van Manen, HJ.; Kraan, Y. M.; Roos, D. and Otto, C. *J. Phys. Chem. B*, **2004,** *108*, 18762–18771.
7. Mahadevan-Jansen, A. and Lieber, C. A. *Appl. Spectrosc*., **2003**, *57,* 1363–1367.